



**Fabrication and Characterization of a Resorbable Barrier Membrane Using  
Silk Fibroin-Fish Collagen Materials**

**Chanokpim Chankum**

**A Thesis Submitted in Partial Fulfillment of the Requirements for the  
Degree of Master of Science in Oral and Maxillofacial Surgery**

**Prince of Songkla University**

**2018**

**Copyright of Prince of Songkla University**

**Thesis Title**            Fabrication and Characterization of a Resorbable Barrier Membrane  
                                   Using Silk Fibroin-Fish Collagen Materials

**Author**                    Miss Chanokpim Chankum

**Major Program**        Oral and Maxillofacial Surgery

---

**Major Advisors**

.....  
 (Assoc. Prof. Prisana Pripatnanont)

**Co-advisor**

.....  
 (Assoc. Prof. Dr. Jirut Meesane)

**Examining Committee:**

.....Chairperson  
 (Prof. Nabil Samman)

.....Committee  
 (Assoc. Prof. Prisana Pripatnanont)

.....Committee  
 (Assoc. Prof. Dr. Jirut Meesane)

.....Committee  
 (Asst. Prof. Dr. Nattawut Theuaksuban)

.....Committee  
 (Assoc. Prof. Dr. Premjit Arpornmaeklong)

The Graduate School, Prince of Songkla University, has approved this thesis as partial fulfillment of the requirements for the Master of Science Degree in Oral and Maxillofacial Surgery.

.....  
 (Prof. Dr. Damrongsak Faroongsarng)

Dean of Graduate School

This is to certify that the work here submitted is the result of the candidate's own investigations. Due acknowledgment has been made of any assistance received.

.....Signature

(Assoc. Prof. Prisana Pripatnanont)

Major Advisor

.....Signature

(Assoc. Prof. Dr. Jirut Meesane)

Co-Advisor

.....Signature

(Miss Chanokpim Chankum)

Candidate

I hereby certify that this work has not been accepted in substance for any degree, and is not being currently submitted in candidature for any degree.

.....Signature

(Miss Chanokpim Chankum)

Candidate

ชื่อวิทยานิพนธ์	การสังเคราะห์และศึกษาคุณลักษณะของแผ่นเยื่อถ่านชนิดสลายตัวได้ที่ผลิตจากซิลิกาไฟโบรอินและคอลลาเจน
ผู้เขียน	นางสาวชนกพิมพ์ จันทร์คำ
สาขาวิชา	ศัลยศาสตร์ช่องปากและแม็กซิลโลเฟเชียล
ปีการศึกษา	2561

## บทคัดย่อ

**วัตถุประสงค์:** แผ่นเยื่อถ่านคอลลาเจนเป็นแผ่นเยื่อถ่านชนิดสลายตัวที่นิยมใช้ในการชักนำให้กระดูกคืนสภาพ อย่างไรก็ตาม แผ่นเยื่อถ่านคอลลาเจนมีการยุบตัว คงรูปร่างไม่ได้ สลายตัวเร็ว ซิลิกาไฟโบรอินจึงถูกนำมาใช้เนื่องจากมีคุณสมบัติเชิงกลที่ดี ก่อให้เกิดการต้านต่อภูมิคุ้มกันน้อย ราคาไม่แพง การศึกษานี้มีวัตถุประสงค์เพื่อสังเคราะห์แผ่นเยื่อถ่านชนิดสลายตัวจากซิลิกาไฟโบรอินและคอลลาเจนจากปลา ซึ่งมีคุณสมบัติเชิงกายภาพ คุณสมบัติเชิงกลเหมาะสม และเข้ากันได้กับเนื้อเยื่อในช่องปฏิบัติการ

**วัสดุและวิธีการ:** แผ่นเยื่อถ่านซิลิกาไฟโบรอินขึ้นรูปจากไหมไทย นำมาเชื่อมกับพอลิเมอร์คอลลาเจนโดยพันธะเคมีข้ามโซ่ นำแผ่นเยื่อถ่านซิลิกาไฟโบรอินไปแช่น้ำก่อนทดสอบคุณสมบัติเชิงกล เพื่อเลือกสูตรในการขึ้นรูป จากนั้นนำไปเชื่อมพอลิเมอร์กับคอลลาเจน แล้วนำแผ่นเยื่อถ่านที่ผลิตขึ้นมาใหม่ไปทดสอบคุณสมบัติเชิงกายภาพและเชิงกล เปรียบเทียบกับแผ่นเยื่อถ่านคอลลาเจนที่มีขายในท้องตลาด โดยคุณลักษณะทางกายภาพของพื้นผิวด้วยกล้องอิเล็กตรอนแบบส่องกราด (SEM) กล้องจุลทรรศน์แรงอะตอม (AFM) การศึกษาหมู่ฟังก์ชันของโมเลกุล (FTIR) การวัดมุมสัมผัสที่ภาวะการแผ่เปียก ค่าเฉลี่ยร้อยละการยึดตัว อัตราการบวมน้ำ และอัตราการสลายตัว ทดสอบความเข้ากันได้ของเนื้อเยื่อโดยใช้เซลล์สร้างกระดูกของหนู (MC3T3-E1) เพื่อศึกษาการยึดเกาะของเซลล์บนแผ่นเยื่อถ่าน ความมีชีวิตของเซลล์ การเพิ่มจำนวนเซลล์ ค่าการดูกลืนแสงจากการสร้างและสะสมแร่ธาตุ การทดสอบทางสถิติโดยโปรแกรม SPSS (Version 16.0, SPSS Inc., Chicago, IL, USA) และทดสอบสมมติฐานทางสถิติแบบ analysis of variance (ANOVA) เปรียบเทียบระหว่างกลุ่มทดสอบ กำหนดให้ผลการศึกษามีนัยสำคัญทางสถิติที่ระดับต่ำกว่า 0.05

**ผลการศึกษา:** การศึกษาลักษณะพื้นผิวของแผ่นเยื่อถ่านด้วยกล้องอิเล็กตรอนแบบส่องกราด (SEM) พบเส้นใยคอลลาเจนบนพื้นผิวของแผ่นเยื่อถ่านซิลิกาไฟโบรอิน-คอลลาเจนเพียงหนึ่งด้าน ต่างจากแผ่นเยื่อถ่านซิลิกาไฟโบรอินซึ่งพบลักษณะพื้นผิวเรียบทั้งสองด้าน การศึกษาด้วยกล้องจุลทรรศน์แรงอะตอม (AFM) พบว่าแผ่นเยื่อถ่านซิลิกาไฟโบรอิน-คอลลาเจนมีลักษณะพื้นผิวที่หยาบกว่าและมีค่าความหยาบของพื้นผิวเท่ากับ 0.2155 ไมโครเมตร ซึ่งมากกว่าแผ่นเยื่อถ่านซิลิกาไฟโบรอินที่มีค่าความหยาบผิวเท่ากับ 0.1424 ไมโครเมตร การศึกษาหมู่ฟังก์ชันของโมเลกุล (FTIR) พบว่าทั้งแผ่นเยื่อถ่านซิลิกา

ไฟโบรอินและแผ่นเยื่อชั้นซิลค์ไฟโบรอิน-คอลลาเจนพบแถบหมู่พันธะเอไมด์ I, II, III และ A การวัดมุมสัมพัทธ์ที่ภาวะการณเป็ยกของแผ่นเยื่อชั้นซิลค์ไฟโบรอิน ( $76.75 \pm 3.07$  องศา) พบว่ามีค่าน้อยกว่าแผ่นเยื่อชั้นซิลค์ไฟโบรอิน-คอลลาเจน ( $112.67 \pm 1.94$  องศา) ซึ่งแสดงถึงพื้นผิวที่ชอบน้ำ ค่าเฉลี่ยร้อยละการยึดตัวของแผ่นเยื่อชั้นซิลค์ไฟโบรอิน ( $28.93 \pm 15.56$  %) มีค่าน้อยกว่าแผ่นเยื่อชั้นซิลค์ไฟโบรอิน-คอลลาเจน ( $42.10 \pm 11.46$  %) และแผ่นเยื่อชั้นคอลลาเจน ( $54.79 \pm 13.44$  %) แต่ไม่มีความแตกต่างอย่างมีนัยสำคัญทางสถิติระหว่างกลุ่มทดสอบ (ค่าพืมากกว่า 0.05) แผ่นเยื่อชั้นคอลลาเจนมีการบวมน้ำสูงกว่า และสลายตัวต่ำกว่ากลุ่มทดสอบอื่นอย่างมีนัยสำคัญทางสถิติ (ค่าพืน้อยกว่า 0.05) ทุกกลุ่มทดสอบพบจำนวนของเซลล์เพิ่มขึ้นอย่างต่อเนื่องคล้ายกันเมื่อเวลามากขึ้น วันที่ 7 ของการศึกษา แผ่นเยื่อชั้นซิลค์ไฟโบรอินพบจำนวนของเซลล์สูงที่สุดระหว่างกลุ่มทดสอบ ( $36,784.17 \pm 2,681.73$  ตัว) ซึ่งสูงกว่ากลุ่มแผ่นเยื่อชั้นซิลค์ไฟโบรอิน-คอลลาเจน ( $15,905.00 \pm 2,148.88$  ตัว) และแผ่นเยื่อชั้นคอลลาเจน ( $12,317.50 \pm 1,267.68$  ตัว) อย่างมีนัยสำคัญทางสถิติ (ค่าพืน้อยกว่า 0.05) วันที่ 21 ของการศึกษา การสร้างและสะสมแร่ธาตุ แผ่นเยื่อชั้นคอลลาเจนพบค่าการดูดกลืนแสงสูงที่สุด แต่ที่วันที่ 28 ของการศึกษาพบว่าแผ่นเยื่อชั้นคอลลาเจน ( $0.78 \pm 0.19$ ) มีค่าการดูดกลืนแสงใกล้เคียงกับแผ่นเยื่อชั้นซิลค์ไฟโบรอิน ( $0.77 \pm 0.13$ ) และมากกว่าแผ่นเยื่อชั้นซิลค์ไฟโบรอิน-คอลลาเจน ( $0.56 \pm 0.04$ ) แต่ไม่พบความแตกต่างอย่างมีนัยสำคัญทางสถิติ (ค่าพืมากกว่า 0.05)

**สรุป:** แผ่นเยื่อชั้นซิลค์ไฟโบรอินและแผ่นเยื่อชั้นซิลค์ไฟโบรอิน-คอลลาเจนที่พัฒนาขึ้นมา มีคุณสมบัติเชิงกายภาพ คุณสมบัติเชิงกล และมีความเข้ากันได้กับเนื้อเยื่อในห้องปฏิบัติการ เหมาะสมกับการทำหน้าที่เป็นแผ่นเยื่อชั้น เพื่อใช้ในการชักนำให้กระดูกคืนสภาพ ควรมีการศึกษาเพิ่มเติมในสัตว์ทดลองเพื่อดูความเข้ากันได้กับเนื้อเยื่อและการทำหน้าที่เป็นแผ่นเยื่อชั้นในร่างกายของสิ่งมีชีวิต

<b>Thesis Title</b>	Fabrication and Characterization of a Resorbable Barrier Membrane Using Silk Fibroin-Fish Collagen Materials
<b>Author</b>	Miss Chanokpim Chankum
<b>Major Program</b>	Oral and Maxillofacial Surgery
<b>Academic Year</b>	2018

## ABSTRACT

**Background:** A collagen membrane had been the most widely used resorbable barrier membrane in guided bone regeneration, however, a membrane was collapsible and had fast degradation. Silk fibroin had been introduced for improving the properties of a membrane due to its high mechanical strength, low immunogenic responses, and economical advantage. This study aimed to fabricate a resorbable barrier membrane using the composite of silk fibroin and fish collagen materials. Physical and mechanical properties, and in vitro biocompatibilities were evaluated.

**Materials and Methods:** A silk fibroin film was made of *Bombyx Mori* silkworm and immobilized with collagen from brown-banded bamboo shark skin by chemical cross-linked. The various ratio of the silk fibroin film was hydrated prior tensile test to select suitable formula before immobilization with collagen. Then, physical and mechanical properties were evaluated to verify the characteristics of a barrier membrane compared with a commercial collagen membrane by using Scanning Electron Microscopy (SEM), Fourier Transform Infrared Spectroscopy (FTIR) and Atomic Force Microscopy (AFM), water contact angles, percentage of elongation, stiffness, swelling degree and degradation degree. In vitro biocompatibility was evaluated in terms of cell attachment and morphology on the membrane, cell viability, cell proliferation and differentiation using MC3T3-E1 cells. The statistical analysis was performed using SPSS software (Version 16.0, SPSS Inc., Chicago, IL, USA). An analysis of variance (ANOVA) was used to compare among experimental groups. The statistical significance was defined as a p-value less than 0.05.

**Results:** The SEM examination demonstrated collagen fibril structure covering silk fibroin-collagen film on the front side and differed from silk fibroin film that showed a non-homogeneous smooth surface on both sides. The AFM demonstrated that silk fibroin-collagen film showed rougher surface and had a higher surface roughness (0.2155  $\mu\text{m}$ ) than silk fibroin film (0.1424  $\mu\text{m}$ ). The FTIR of both silk fibroin film and silk fibroin-collagen film showed the spectrum of peptide bonds of Amide I, II, III and A. The silk fibroin film demonstrated fewer contact angles

( $76.75^\circ \pm 3.07$ ) than silk fibroin-collagen film ( $112.67^\circ \pm 1.94$ ), referred to the more hydrophilic surface. The average percentage of elongation of the silk fibroin film ( $28.93 \pm 15.56$ ) was less than the silk fibroin-collagen film ( $42.10 \pm 11.46$ ) and Bio-Gide<sup>®</sup> collagen membrane ( $54.79 \pm 13.44$ ) but showed no statistical significance among groups ( $p$ -value  $> 0.05$ ). The commercial collagen membrane exhibited significantly higher swelling degree and had slower degradation than other groups ( $p$ -value  $< 0.05$ ). All study groups showed a similar pattern of cell proliferation that continuously increased with time in all groups. The silk fibroin film had significantly highest cell numbers ( $36,784.17 \pm 2,681.73$ ), which was higher than silk fibroin-collagen film ( $15,905.00 \pm 2,148.88$ ) and Bio-Gide<sup>®</sup> collagen membrane ( $12,317.50 \pm 1,267.68$ ) and showed statistical significance ( $p$ -value  $< 0.05$ ) on culture Day 7. The result of mineralization on culture Day 21, collagen membrane was higher than other groups. On culture Day 28, collagen membrane ( $0.78 \pm 0.19$ ) were in the same level as silk fibroin film ( $0.77 \pm 0.13$ ) and higher than silk fibroin-collagen film ( $0.56 \pm 0.04$ ) but showed no statistical significance ( $p$ -value  $> 0.05$ ).

**Conclusion:** The in-house silk fibroin film and silk fibroin-collagen film had been developed at an economic cost and possessed physical, mechanical and in vitro biocompatibility properties of a barrier membrane used for GBR. Further study on biocompatibility and the barrier efficacy in vivo should be performed.



## ACKNOWLEDGMENTS

This thesis would not have been accomplished without the support, guidance, and help from others. I am especially thankful to my principal supervisor Assoc. Prof. Prisana Pripatnanont who is my role model and always encourage, supervise and support me with her kindness, patience, and knowledge throughout my thesis. I am the most grateful for her advice which is not only the research but also clinical practice and lifestyle.

I would like to sincerely thank my supervisor Assoc. Prof. Dr. Jirut Meesane who have instructed me the new knowledge advised great opinion and supported me throughout this thesis.

I would also like to thank Miss Khanitta Panjapheree and Miss Supaporn Sangkert, staffs from the Institute of Biomedical Engineering at the Faculty of Medicine, Prince of Songkla University and all the staffs of the Department of Oral and Maxillofacial Surgery at the Faculty of Dentistry, Prince of Songkla University and for their help and support throughout this thesis.

Finally, I must express my very appreciation to my parents who are everything to me, to my brother and to my friends for providing me all support and continuous encourage me throughout my years of study and process of the research. This thesis would not have been completed or written without them. Thank you so much.

Chanokpim Chankum

## CONTENTS

	<b>Page</b>
Abstract (Thai language) .....	v
Abstract (English language) .....	vii
Contents.....	x
List of Tables.....	xi
List of Figures.....	xii
List of Abbreviations and Symbols.....	xiv
Chapter	
1. Introduction.....	1
2. Materials and Methods.....	12
Phase I: Fabrication of a resorbable barrier membrane.....	12
Phase II: Characterization with physical and mechanical properties.....	17
Phase III: In vitro biocompatibility evaluation .....	21
3. Results.....	24
4. Discussion.....	41
5. Conclusion.....	48
References list.....	49
Appendix.....	56
Vitae.....	57

## LIST OF TABLES

<b>Tables</b>	<b>Page</b>
Table 1. Membranes used for guided bone regeneration (GBR) .....	3
Table 2. Comparison of non-resorbable with resorbable membrane .....	6
Table 3. Summary of the commercially available membrane for guided bone regeneration .....	7
Table 4. Summary the structure of silk fibers .....	8
Table 5. Description of study groups .....	12
Table 6. Measurement variables .....	23
Table 7. The surface roughness (RMS) of barrier membranes .....	28
Table 8. The contact angle of samples .....	30
Table 9. Maximum elongation and percentage of elongation of experimental groups.....	31
Table 10. The stiffness of experimental groups .....	32
Table 11. Swelling degree of experimental groups.....	33
Table 12. Degradation degree of experimental groups .....	35
Table 13. Cell proliferation numbers of experimental groups .....	38
Table 14. Optical density (OD) of experimental groups.....	40

## LIST OF FIGURES

<b>Figures</b>	<b>Page</b>
<b>Figure 1.</b> Illustration scheme of the guided bone regeneration or (GBR).....	3
<b>Figure 2.</b> Illustration scheme of the guided bone regeneration procedure .....	4
<b>Figure 3.</b> Illustration scheme of the silk fibroin structure .....	8
<b>Figure 4.</b> Picture of silk and degummed silk fibroin.....	13
<b>Figure 5.</b> Picture of freeze-dried acid-soluble collagen (ASC) from brown-banded bamboo shark skin .....	13
<b>Figure 6.</b> Picture of commercial collagen membrane (Bio-Gide <sup>®</sup> ).....	13
<b>Figure 7.</b> Picture of degummed silk fibroin and silk fibroin aqueous solution.....	14
<b>Figure 8.</b> Picture of 10% w/v silk fibroin aqueous solution mixed with 3% glycerol .....	14
<b>Figure 9.</b> Picture of silk fibroin film .....	15
<b>Figure 10.</b> Picture of silk fibroin film which was fixed with acrylic frame and immersed in methanol .....	15
<b>Figure 11.</b> Picture of silk fibroin film which was dipped in collagen.....	16
<b>Figure 12.</b> The mechanism of EDC/NHS .....	16
<b>Figure 13.</b> Photograph of FEI Quanta 400 machine.....	17
<b>Figure 14.</b> Photograph of Bruker EQUINOX 55 .....	18
<b>Figure 15.</b> Photograph of OCA 15EC .....	18
<b>Figure 16.</b> Photograph of Nanosurf easy scan 2 .....	19
<b>Figure 17.</b> Photograph of LRXPlus universal testing machine.....	19
<b>Figure 18.</b> Illustration of sample size.....	20
<b>Figure 19.</b> Pictures of front side and back side of the silk fibroin film.....	24
<b>Figure 20.</b> Pictures of front side and back side of the silk fibroin-collagen film.....	24
<b>Figure 21.</b> Pictures of fibrous surface and dense surface of commercial collagen membrane .....	25
<b>Figure 22.</b> Mean thickness of experimental groups .....	25
<b>Figure 23.</b> SEM photograph of experimental groups.....	26
<b>Figure 24.</b> The 3D of AFM photograph of the front side and back side of silk fibroin film .....	27
<b>Figure 25.</b> The 3D of AFM photograph of the front side and back side of silk fibroin-collagen .....	27

**LIST OF FIGURES (CONTINUED)**

<b>Figures</b>	<b>Page</b>
<b>Figure 26.</b> The infrared absorption spectrum of experimental groups.....	28
<b>Figure 27.</b> Pictures of contact angle of silk fibroin film and silk fibroin-collagen film .....	30
<b>Figure 28.</b> Mean contact angle of silk fibroin film and silk fibroin-collagen film .....	30
<b>Figure 29.</b> Mean percentage of elongation of experimental groups.....	32
<b>Figure 30.</b> Mean stiffness of experimental groups .....	33
<b>Figure 31.</b> Mean swelling degree of experimental groups .....	34
<b>Figure 32.</b> Mean degradation degree of experimental groups.....	35
<b>Figure 33.</b> The SEM photograph of cell morphology .....	36
<b>Figure 34.</b> Pictures of viability of experimental groups.....	37
<b>Figure 35.</b> Mean cell proliferation numbers of experimental groups.....	39
<b>Figure 36.</b> Mean optical density of experimental groups.....	40
<b>Figure 37.</b> Reaction scheme for surface modification of silk fibroin film by the collagen solution .	46

**LIST OF ABBREVIATIONS AND SYMBOLS**

<b>AFM</b>	=	Atomic Force Microscopy
<b>Ala</b>	=	Alanine
<b>ALP</b>	=	Alkaline phosphatase
<b>ANOVA</b>	=	One-way analysis of variance
<b>ASC</b>	=	Acid-soluble collagen
<b>ATR</b>	=	Attenuated Total Reflectance
<b>β-sheet</b>	=	Beta sheet
<b>cm<sup>2</sup></b>	=	Centimeter squared
<b>CO<sub>2</sub></b>	=	Carbon dioxide
<b>d-PTFE</b>	=	Dense polytetrafluoroethylene
<b>EDC</b>	=	Ethyl dimethyl aminopropyl carbodiimide
<b>e-PTFE</b>	=	Expanded polytetrafluoroethylene
<b><i>et al</i></b>	=	and others
<b>FBS</b>	=	Fetal bovine serum
<b>FTIR</b>	=	Fourier Transform Infrared Spectroscopy
<b>GBR</b>	=	Guided bone regeneration
<b>Gly</b>	=	Glycine
<b>HCL</b>	=	Hydrochloride
<b>KBr</b>	=	Potassium bromide
<b>kDa</b>	=	Kilodalton
<b>kV</b>	=	Kilovolt
<b>M</b>	=	Molar
<b>min</b>	=	Minutes
<b>mg</b>	=	Milligram
<b>ml</b>	=	Milliliter
<b>mm</b>	=	Millimeter

**LIST OF ABBREVIATIONS AND SYMBOLS (CONTINUED)**

<b>Na<sub>2</sub>CO<sub>3</sub></b>	=	Sodium carbonate
<b>nm</b>	=	Nanometer
<b>NSH</b>	=	N-hydroxysuccinimide solution
<b>OD</b>	=	Optical density
<b>PBS</b>	=	Phosphate-buffered saline solution
<b>pH</b>	=	Potential of Hydrogen ion
<b>RMS</b>	=	Root Mean Square
<b>Rpm</b>	=	Revolutions per minute
<b>SBF</b>	=	Simultaneous body fluid
<b>SEM</b>	=	Scanning Electron Microscope
<b>Ser</b>	=	Serine
<b>SF</b>	=	Silk fibroin
<b>SG</b>	=	Silk fibroin with 3% glycerol film
<b>SG-Col</b>	=	Silk fibroin with 3% glycerol - collagen film
<b>wt%</b>	=	Weight percent
<b>w/v</b>	=	Weight per volume
<b>°</b>	=	Degree
<b>°C</b>	=	Degree Celsius
<b>μm</b>	=	Micrometer
<b>α-MEM</b>	=	Alpha-Minimum Essential Medium

## CHAPTER 1

### INTRODUCTION

#### **Background:**

Nowadays, the application of barrier membranes in guided bone regeneration (GBR) technique has become a popular surgical technique in ridge augmentation. An expanded polytetrafluoroethylene (e-PTFE), a non-resorbable barrier membrane, was a famous barrier membrane in GBR in the earliest time. Although clinical and experimental studies of using an e-PTFE membrane had shown excellent treatment results (1, 2), the outcome was jeopardized by wound healing complications, especially soft tissue dehiscence (3, 4). Many studies had reported wound infection following the exposure of an e-PTFE membrane and consequently a poor outcome in bone regeneration (5, 6). Moreover, an e-PTFE membrane had to be removed, thus the patients have to undergo a secondary procedure that leads to discomfort, increased cost and risk of losing some of the regenerated bone. A resorbable barrier membrane is well accepted and more preferable to a non-resorbable barrier membrane because it does not require the secondary surgical procedures to remove it. A collagen barrier membrane has been the most popular application which was used and offers several advantages, such as biocompatibility and bioresorbability (7, 8). On the other hand, a collagen membrane has high cost and also been reported of many drawbacks for large and vertical bone augmentation such as unfavorable mechanical properties, inadequate barrier membrane durability in wet condition and short degradation time (9-13).

The desired properties of the barrier membrane for GBR must follow these criteria that are good in cell-occlusion properties, biocompatibility, space-making ability, clinical manageability, integration with surrounding tissues, favorable mechanical and physical properties, and low cost. Silk from the *Bombyx mori*, silkworm was chosen to use as a biomedical suture material for eras (14). Recently, silk fibroin is one of the popular materials used in tissue engineering, which has been used as scaffolding for new tissue regeneration (15-19) because of its mechanical properties including high strength, toughness, environmental stability, biocompatibility and biodegradability (20). Silks are defined as protein polymers which could be spun into fibers by silkworms, flies, spiders, mites, and scorpions in general (14). Silk fibroin can be processed into a variety of forms such as fibers (17, 21), sponges (16, 17, 21), hydrogels (17, 21), and films (17, 20, 21). Therefore, the



silk fibroin membrane also has been considered to use as a barrier membrane for guided bone regeneration technique. Silk fibroin membrane is a good option for the popular collagen membrane in the guided bone regeneration (GBR) due to silk fibroin membranes could enhance new hard tissue formation in a rat calvarial defect model without inflammatory tissue reaction and result in similar volumes of new bone formation when compared with a collagen membrane (22). However, pure silk fibroin membranes are brittle and stiff when keeping at room temperature over time. Therefore, silk fibroin membranes need to be modified in terms of the mechanical and physical properties to gain more flexible.

The purpose of the present research was to fabricate the new resorbable barrier membrane that possesses favorable barrier membrane properties by using silk fibroin and fish collagen as materials. Physical and mechanical properties were assessed to confirm the characteristics of a barrier membrane for the guided bone regeneration (GBR) technique in ridge augmentation and compared with an available commercial collagen membrane. Therefore, the new resorbable barrier membrane could be fabricated at an economic cost and possess the properties of a barrier membrane used for GBR as follows; biocompatibility, cell occlusion, tissue integration, space making and space maintenance, easy clinical handling during surgery and limited susceptibility to complication.

#### **Literature reviews:**

The principle of guided bone regeneration (GBR) technique is a surgical procedure that using resorbable or non-resorbable barrier membranes for excluding rapidly connective tissue and proliferating epithelium thus boosting the proliferation and differentiation of slower-growing cells capable of forming bone with or without combined particulate bone grafts or/and bone substitutes (23) as shown in *Figure 1*.

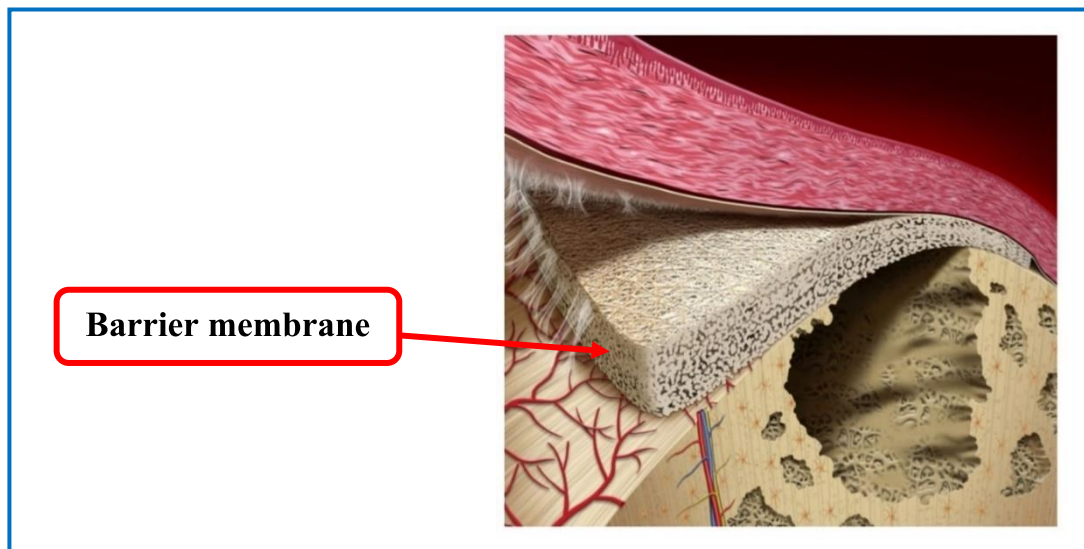


**Figure 1.** Illustration scheme of the guided bone regeneration or GBR (24)

The barrier membranes should possess the following properties for GBR; cell exclusion, tenting, scaffolding, stabilization, and framework (24). The basic requirements of the biomaterial include biocompatibility, cell occlusion, tissue integration, space making and space maintenance, easy clinical handling during surgery and limited susceptibility to complication (25). The barrier membranes can be classified as a non-resorbable barrier membrane; which typically needs to be removed and a resorbable barrier membrane; which is hydrolyzed or enzymatically degraded and therefore do not require a second surgical procedure of membrane removal. The resorbable barrier membrane is then divided as a natural membrane or a synthetic membrane depending on their origin as shown in *Table 1* (26).

**Table 1.** Membranes used for guided bone regeneration (GBR) (26)

Non-resorbable	Resorbable	
	Natural	Synthetic
<b>Polytetrafluoroethylene</b> e-PTFE d-PTFE	Native collagen Cross-linked collagen	<b>Polymers</b> Polyglactin Polyurethane Polylactic acid Polyglycolic acid Polyethylene glycol

**Table 1.** (Continued)

Non-resorbable	Resorbable	
	Natural	Synthetic
<b>Metals</b>	Extracellular matrices derived from bovine, porcine and human tissues	<b>Inorganic compounds</b> Calcium sulfate Calcium phosphate (e.g. hydroxyapatite)
Titanium and titanium alloys		
Cobalt-chromium alloy		
	Chitosan	
	Silk fibroin	

\* e-PTFE, expanded polytetrafluoroethylene; d-PTFE, dense polytetrafluoroethylene

Several clinical research demonstrated that GBR was a favorable and prosperous technique for horizontal bone augmentation (*Figure 2*) and could be done successfully using either non-resorbable or resorbable membranes (27, 28)

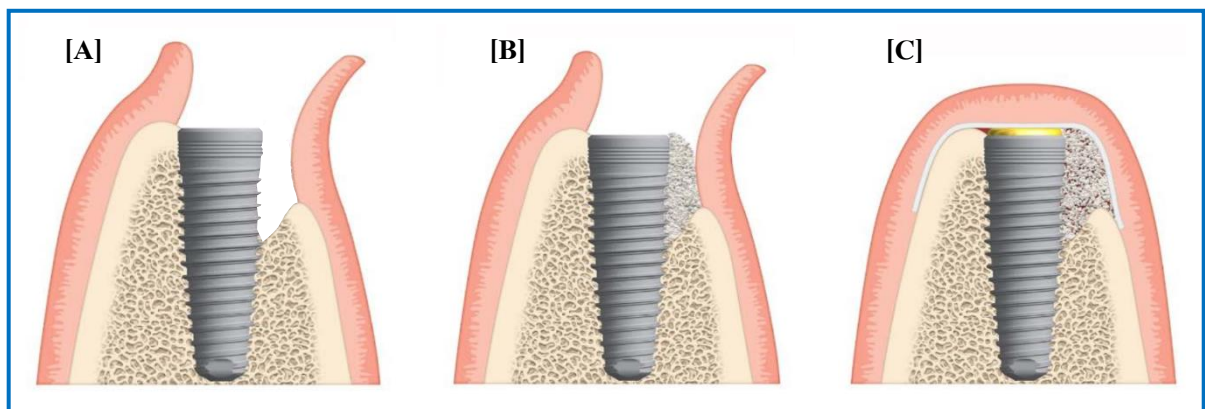


**Figure 2.** Illustration scheme of the guided bone regeneration procedure: (A) the horizontal bone defect, (B) fill the defect with autologous bone chips on the implant surface and an organic bovine bone matrix on top, (C) cover the defect and implant site with the collagen membrane, which modified from (28).

An expanded polytetrafluoroethylene (e-PTFE) membrane, a non-resorbable barrier membrane, has been proved to be effective in preventing connective tissue and epithelial tissue invasion of the healing area and presenting regeneration of bone (4, 29-31). Previous clinical study of using a collagen membrane (Bio-Gide<sup>®</sup>) versus e-PTFE membrane with demineralized bovine bone mineral (Bio-Oss<sup>®</sup>) and a follow-up period of 5 years and 12-14 years after GBR and reported the mean marginal bone level was higher in the e-PTFE group than collagen membrane group but no significant difference was found between them (32, 33). The application of an e-PTFE barrier

membrane for augmentation of horizontal bone deficiency by guided bone regeneration (GBR) technique in the anterior maxilla was done and gave good clinical outcome after 1 year in function (23). Besides the need for membrane removal, the non-resorbable barrier membranes also had disadvantages of membrane exposure, which has been a frequent postsurgical complication (4, 34).

At present, the available resorbable barrier membranes are either made from natural materials such as collagen, chitosan and silk fibroin or synthetic polymers such as polylactic acid/polyglycolic acid copolymer (PLGA). A collagen membrane is a natural resorbable barrier membrane and has been the most widely used and offers several advantages, such as excellent biocompatibility (7, 8), low antigenicity (7, 8, 35), bioresorbability (36) and high level of direct cell adhesion (37). Not only it is not suitable for large augmentation due to weak tensile strength in the wet state, but also it is expensive. In vivo study, a collagen membrane was nearly completely biodegraded in 4 weeks (13). A collagen membrane has less stiffness compared with a non-resorbable membrane such as a titanium membrane or an expanded polytetrafluoroethylene (e-PTFE) in general use with patients. Thus, the space maintaining ability of a collagen membrane was lower than that of an e-PTFE membrane or a titanium mesh. Additionally, a cross-linking collagen membrane was related with slow biodegradation, less tissue integration, less vascularization, and foreign body reactions, while non-crosslinked collagen barrier membrane has shown perfect tissue integration, fast vascularization, and no foreign body reaction. Moreover, glutaraldehyde cross-linking could inhibit the proliferation and attachment of fibroblasts and osteoblasts (13). Comparison of advantages and disadvantages between the non-resorbable barrier membrane and the resorbable barrier membrane was shown in *Table 2* (38).

**Table 2.** Comparison of non-resorbable with a resorbable membrane

	<b>Non-resorbable</b>	<b>Resorbable</b>
<b>Advantages</b>	Maintains space well Reliable bone regeneration Inert and stable polymer High toughness and plasticity	Does not require removal Integrates with body Pliable and shapeable Exposure may close spontaneously Bioresorbability Low immunogenicity Drug-encapsulating ability
<b>Disadvantages</b>	Requires removal Does not integrate The possible higher exposure rate Must be removed if exposed, resulting in less regeneration	Collapsible May trigger an immune response May disintegrate faster than desired Less well studied Less effective for vertical defects Less occlusive (more fibrous tissue ingrowth)

Nowadays, the collagen membrane is the most popular commercial resorbable membrane. Generally, the main source of collagen isolation was from porcine or bovine. Collagen from mammalian source has been utilized as biomaterials in the medical applications and has the advantage of biodegradability (39). However, the outbreak of mad cow disease or bovine spongiform encephalopathy (BSE) cause anxiety among users of bovine collagen due to some reports have shown the transmission risk of bovine spongiform encephalopathy to human beings (40). In addition, the porcine collagen could not be used in some countries because of religious confinement (39). Recently, non-mammalian collagen sources especially in fish collagen, such as sharks and salmons skin were interesting as having a low risk for transmission of infectious disease to humans than bovine collagen, and no religious restriction. (40)

**Table 3.** Summary of the commercially available membrane for guided bone regeneration (41)

Product	Raw materials	Cross-linking	Biodegradation
Alloderm	Acellular dermal matrix	Not presented	Yes
Bio-Arm	Porcine type I collagen	Yes (formaldehyde)	Yes
Bio-Gide	Porcine type I and III collagen	No	Yes
Biomend	Bovine type I collagen	Yes (glutaraldehyde)	Yes
Cytoblast RTM collagen	Bovine type I collagen	Not presented	Yes
EZ cure	Porcine type I and all collagen	Yes	Yes
Guidos	Porcine type I collagen	Yes	Yes
OSSIX plus	Porcine-based collagen	Yes (sugar based)	Yes
OsseoGuard Flex	Bovine type I and all collagen	Yes	Yes
Lyoplant	Bovine collagen	No	Yes
Rapiderm	Porcine type I collagen	Not presented	Yes
Rapigide	Porcine type I collagen	Not presented	Yes
Surederm	Human skin tissue	Not presented	No
Cytoflex (open membrane TEF guard)	Micro-porous, PTFE membrane	No	No
Cytoplast (Ti-250 or Ti 150 Titanium-Reinforced)	High-density PTFE membrane	No	No
Cytoplast TXT200	High-density PTFE membrane	No	No
Gore-TEX	Expanded PTFE membrane	No	No
Open-tex	High-density PTFE membrane	No	No

\* PTFE; polytetrafluoroethylene

Recently, silk fibroin is one of the popular materials used in tissue engineering because of its mechanical properties including high strength, toughness, environmental stability, biocompatibility and biodegradability (20). The structure, properties, and composition of silk protein depend on their sources. Silk from *Bombyx mori* (silkworm) has been used as a biomedical suture material for centuries (14). Summary the structure of silk fibers is shown in *Table 4*. Silk is comprised of two proteins which are fibroin and sericin as shown in *Figure 3*. The silk fibroin fiber is water-insoluble which is composed of a heavy chain and a light chain, which are connected by a disulfide bond as well as a glycoprotein named P25 (42). While the glue-like sericin which has a high content of hydrophilic amino acids is involved in immunological reactions and induces an allergic reaction. So, sericin should be removed before using as biological applications (16-19). Silk fibroin is approved by the American Food and Drug Administration (FDA) as a source for biomaterials production. Silk

fibroin materials with film structures typically prepared by casting technique (43). The stability of silk fibroin film which used as biomaterial can be improved by alcohol immersion (44), stretching (45) and slow-drying (46). The previous study reported that water-insoluble silk fibroin films which were treated by immersion in methanol or ethanol for increasing  $\beta$ -sheet content resulted in high water vapor and oxygen permeability, and good mechanical properties (43).

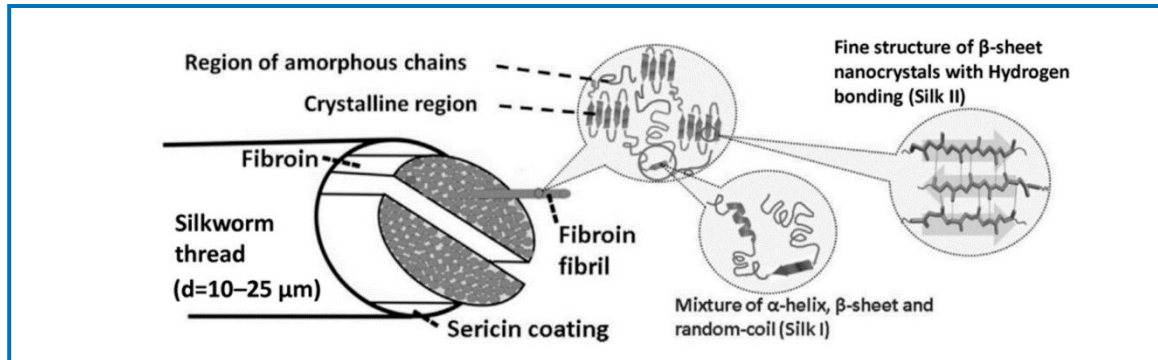


*Figure 3. Illustration scheme of the silk fibroin structure (47).*

**Table 4.** Summary the structure of silk fibers (42)

Silkworm	Composition	Molecular weight	Structures
Silk Fibroin (~70 wt%)	Heavy chain fibroin	390 kDa	- (Gly-Ala-Gly-Ala-Gly-Ser) <sub>n</sub> - To form anisotropic $\beta$ -sheet rich nanocrystals
	Light chain fibroin	26 kDa	- Linked by a disulfide bond - Hydrophilic and relatively elastic
	P25 glycoprotein	30 kDa	- Non-covalent hydrophobic interactions - Maintaining the integrity of the complex
Sericin (~20-30 wt%)	A glue-like glycoprotein	20-310 kDa	- Coating protein - Antigenic protein

Silk fibroin membrane reported that had biocompatibility by examination of cell proliferation, morphology, and differentiation of MC3T3-E1 cells on membrane compared with the culture dishes (48). Comparison of efficacy between silk fibroin and collagen membrane revealed that new hard tissue formation in a rat skull defect model could be enhanced successfully without any adverse inflammatory reactions by using silk fibroin membranes for GBR. Similar volumes of bone

regeneration and low risk of infectious transmission from animal tissue was observed when collated with the collagen membrane. The previous study recommended that silk fibroin membrane was a good alternative to the widely used collagen membrane in the guided bone regeneration (GBR) (22).

In the pilot study, silk fibroin film and silk fibroin-collagen film were fabricated and evaluated as a barrier membrane. The silk fibroin-collagen film was more bending than silk fibroin film but both of fabricated barrier membranes were brittle and dry at room temperature over time. Silk fibroin film without collagen immobilization had smooth surface by gross observation and showed no porosity on both sides. Moreover, collagen fibrils could be self-assembly immobilized on silk fibroin films and had been shown different morphology when analyzed with scanning electron microscopy (SEM) and atomic force microscopy (AFM). Immobilized collagen on silk fibroin film showed rougher surface of nanoscale roughness in comparison with silk fibroin film because of collagen immobilization on the surface of silk fibroin film when assessed by using atomic force microscopy (AFM). While the surfaces of the Bio-Gide<sup>®</sup> collagen membrane were different. One side had a rough surface with some fibers when the other side had a dense smoother surface by gross observation.

The outcome of FTIR spectroscopy analysis revealed that the spectrum of a protein was composed of many vibrational bands arising from different functional groups. The major absorption bands of collagens were in the amide band region. The peak of amide I, amide II, amide III, amide A and amide B were found in this study. On the other hand, the peak of amide IV which was represented sericin was not found in this study because silk was degummed during silk fibroin film preparation and sericin was removed.

The hydrophobic-hydrophilic properties of a new barrier membrane surface were different between silk fibroin film with and without collagen immobilization. Self-assembly collagen on silk fibroin film changed surface properties from hydrophilic surface to hydrophobic surface. This could be explained that the hydrogen bonding formation induces the cross-linking of silk fibroin and collagen and by turn the hydrophobic of the films.

Mechanical properties in term of ductility of barrier membrane could be assessed by evaluation of a percentage of elongation. Silk fibroin-collagen film showed less percentage of elongation than other groups but still had increasing elongation property at around 27 percent from initial gauge length which might suffice for use a barrier membrane. In term of stiffness represented rigidity of a barrier membrane which resists deformation in response to an applied force, silk fibroin-collagen film demonstrated the highest stiffness than other groups which referred to the less flexible



barrier membrane. The in-house silk fibroin-collagen film should be improved to fit physical and mechanical properties of a barrier membrane used for GBR technique such as more flexibility, a hydrophilic surface, and biocompatibility.

In the present study, the flexible silk fibroin membranes would be developed by blending glycerol with silk fibroin aqueous solution before casting. Glycerol is a hydrophilic plasticizer which is appropriate for dosage forms formulation according to the 35<sup>th</sup> edition of the United States Pharmacopoeia in 2011. There are many criteria for selecting plasticizer in medicine and pharmacy such as biocompatibility, plasticizer effect on drug release and mechanical properties, plasticizer compatibility with a given polymer, processing characteristics, mode of administration, dosing frequency, dosage size and cost-benefit analysis (49). The concentrations of the plasticizer in the polymer usually range from 5% to 30%, but some study existed deviations from this range. Other studies showed that adding glycerin ranged 1% to 5% or ethanol or both in the dialyzed silk fibroin solution. The addition of glycerin and/or ethanol-induced the formation of films that were presented a significant improvement in the elongation values when compared to the pure silk fibroin film (50, 51). It was found that addition of glycerol to silk fibroin film increased the elongation at break both in dry and wet states because of the plasticizer properties of glycerol that applied in other materials for gaining higher flexibility (50). Moreover, the membranes were not toxic to cells, indicating that they are materials with the potential to be applied as biomaterials (51) However, blending glycerol with silk fibroin aqueous solution before casting silk fibroin membrane remains a challenge to control mechanical properties. Therefore, this study explored alternative plasticizer options, in particular, glycerol.

The MC3T3-E1 cells are a popular pre-osteoblast cell type derived from calvarium of a newborn mouse with an adherent growth property. These MC3T3-E1 cells are good models for observation in vitro osteoblast proliferation and differentiation due to similar behavior to primary calvarial osteoblasts. The MC3T3-E1 cells have the ability to differentiate into osteoblasts, osteocytes and calcified bone tissue forming in vitro (52). The MC3T3-E1 cells have advantages such as a homogenous character, limitless number of cells, phenotypic differentiation from pre-osteoblasts to mature osteoblasts (52-54). On the other hand, they also have disadvantages such as interspecies deviation and cellular replicative senility signs (55). Cells proliferation in vitro and type I collagen synthesis could be assessed from day 3 in cell culture. ALP enzyme activity increased from day 3 to day 21 at the same time while the mineral deposition was presented early at day 14 (54).

**Research question:**

Did a new resorbable barrier membrane made of silk fibroin and fish collagen gain proper physical and mechanical properties as a barrier membrane for guided bone regeneration technique?

**General objective:**

To fabricate a new resorbable barrier membrane using silk fibroin-fish collagen materials.

**Specific objectives:**

1. To fabricate a new resorbable barrier membrane using silk fibroin-fish collagen material.
2. To evaluate physical properties in term of morphology, surface topography, roughness and contact angles of a new fabricated resorbable barrier membrane.
3. To evaluate mechanical properties in terms of percentage of elongation, stiffness, swelling degree and degradation degree of a new fabricated resorbable barrier membrane.
4. To evaluate biocompatibility properties in terms of cell attachment, cell morphology, cell viability, cell proliferation, and mineralization.

**The benefit of this study:**

1. The successful in-house resorbable barrier membrane will be used clinically as a barrier membrane in the Guided Bone Regeneration (GBR) technique for ridge augmentation.
2. To reduce the cost of imported products from outside the country and for patients.
3. To provide the scientific knowledge of a resorbable barrier membrane using silk fibroin-fish collagen material.
4. The in-house resorbable barrier membrane will be modified and applied for use in the other parts of the human body for medical reasons.
5. To construct a protocol to develop a clinical grade of a resorbable membrane based on silk fibroin.

## CHAPTER 2

### MATERIALS AND METHODS

#### Research design:

The study was experimental in vitro study comprised of 3 phases.

#### Phase I: Fabrication of a resorbable barrier membrane

#### Phase II: Characterization with physical and mechanical properties

#### Phase III: In vitro biocompatibility evaluation

**Phase I:** There were two fabricated groups of material as follows.

**Group A;** Silk fibroin film

**Group B;** Silk fibroin-collagen film

These two groups would be constructed and compared with **Group C** which was a commercial porcine collagen resorbable membrane (Bio-Gide<sup>®</sup> Geistlich, Switzerland).

**Table 5.** Description of study groups

Group of study	Descriptions	Abbreviation
A	Silk fibroin with 3% glycerol film	SG
B	Silk fibroin with 3% glycerol - collagen film	SG-Col
C	Commercial collagen resorbable membrane (Bio-Gide <sup>®</sup> Geistlich, Switzerland)	Collagen

First, a new resorbable barrier membrane would be constructed using a casting technique into silk fibroin with glycerol film.

#### 1.1 Preparation of materials

##### Silk fibroin from *Bombyx mori*. silk cocoons

Silk (*Figure 4.A*) were cut into small size and degummed by boiling in 0.02 M Na<sub>2</sub>CO<sub>3</sub> for 30 minutes at room temperature. Then, degummed silk was rinsed against distilled water to remove sericin and would be dried at room temperature overnight (*Figure 4.B*).

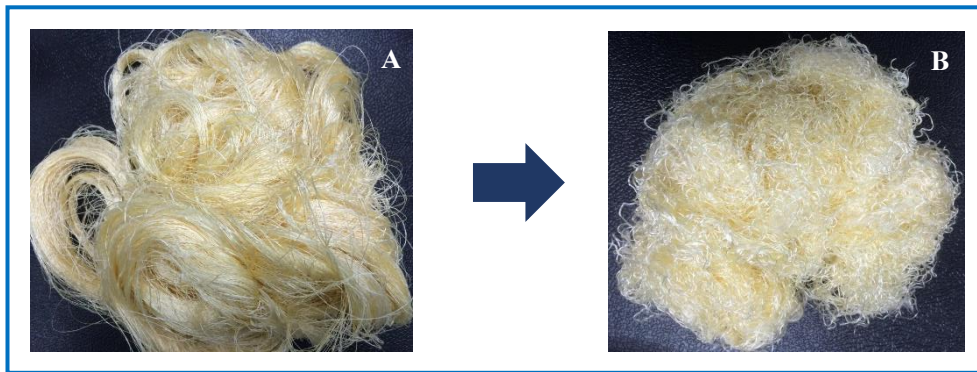


**Figure 4.** Picture of silk (A) and degummed silk fibroin (B)

#### **Collagen from shark skin (*Carcharodon carcharias*)**

Freeze-dried acid-soluble collagen (ASC) (Figure 5) was extracted from shark skin (56), which was prepared by the Department of biomaterials and tissue engineering, Faculty of Medicine, Prince of Songkla University, Songkhla, Thailand.

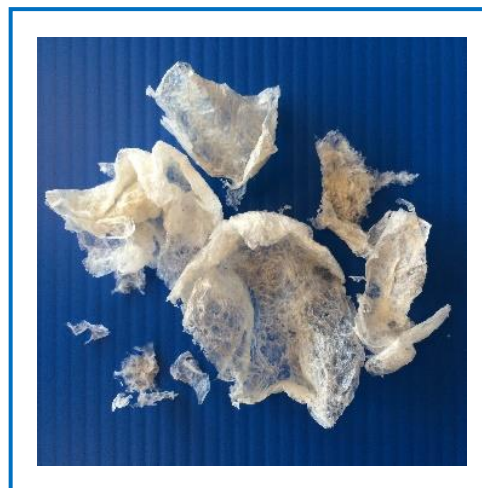


**Figure 5.** Picture of freeze-dried acid-soluble collagen (ASC) from brown-banded bamboo shark skin

#### **Commercial porcine collagen resorbable membrane (Bio-Gide<sup>®</sup> Geistlich, Switzerland)**

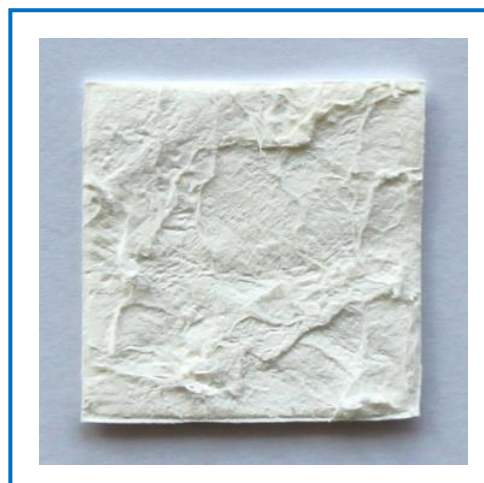


**Figure 6.** Picture of commercial collagen membrane (Bio-Gide<sup>®</sup>)

## 1.1 Methods

### 1.1.1 Fabrication of silk fibroin film

First, 10% w/v silk fibroin aqueous solution (*Figure 7.B*) was prepared by dissolved silk fibroin (*Figure 7.A*) in 9.3 M LiBr solution at 60°C for 4 hours. Then, silk fibroin aqueous solution was dialyzed with a cellulose membrane against distilled water for 72 hours and changed the distilled water every 6 hours to remove LiBr. After that, the silk fibroin solution was centrifuged at 3,000 rpm for 20 minutes and keep at 4°C (20).



**Figure 7.** Picture of degummed silk fibroin (A) and silk fibroin aqueous solution (B)

Second, 10 % w/v silk fibroin aqueous solution mixed with 1 % or 3 % glycerol would be rinsed to a plastic plate to obtain a silk fibroin film. Mechanical and physical properties would be tested to select only one formula of glycerol for using in Group A and B. And, 3 % glycerol was selected and mixed with 10 % w/v silk fibroin aqueous solution (*Figure 8.A*) to make a total volume 3 mL and then, was rinsed to a plastic plate size 3.5 mm x 3.5 mm (*Figure 8.B*) by casting technique and dried at room temperature for 48 hours to obtain a silk fibroin film (*Figure 9*).

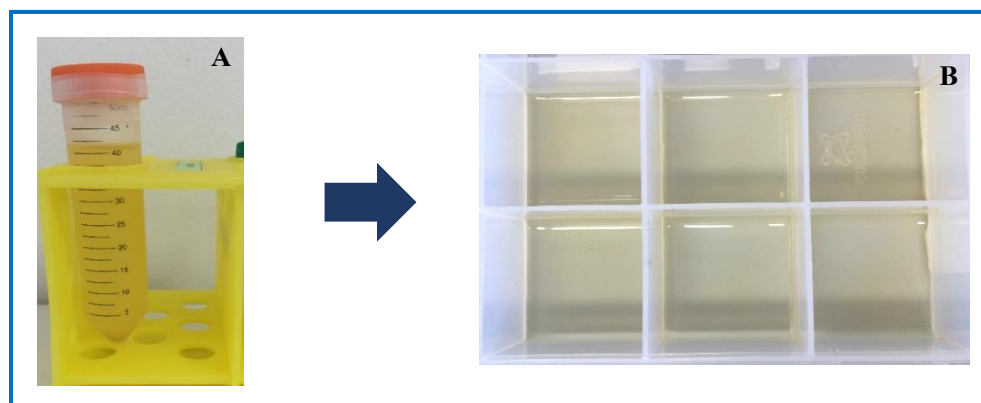


**Figure 8.** Picture of 10% w/v silk fibroin aqueous solution mixed with 3% glycerol (A) which was rinsed to a plastic plate (B)

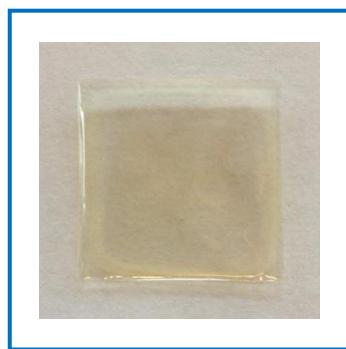


**Figure 9.** Picture of silk fibroin film

### 1.1.2 Surface modification and immobilization of collagen on silk fibroin film

Selected silk fibroin film was fixed with a plastic frame (*Figure 10.A*). Then, the silk fibroin film was immersed in 80% methanol for 20 minutes for inducing  $\beta$ -sheet formation and immerse in 60% methanol for 20 minutes for preventing film shrinkage (*Figure 10.B*). Then, the silk fibroin film was hydrated in phosphate-buffered saline solution (PBS) of pH 7.4 at room temperature for 30 minutes (20).

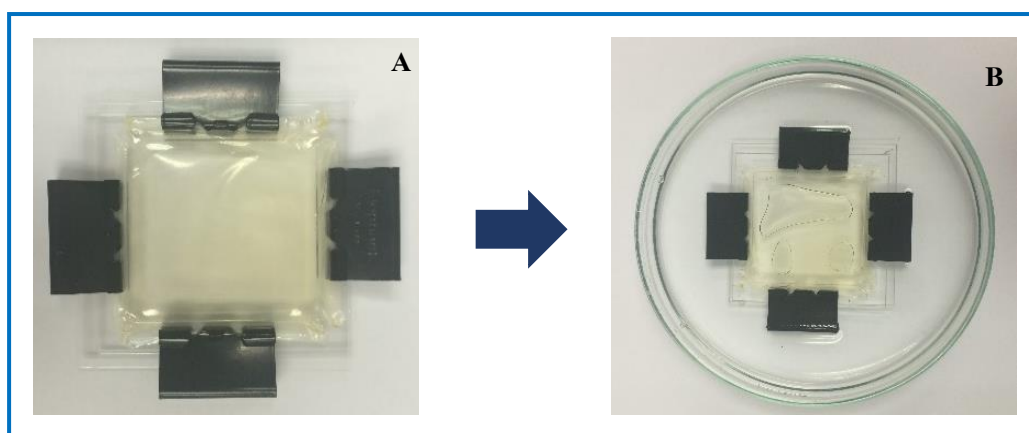


**Figure 10.** Picture of silk fibroin film which was fixed with the acrylic frame (A) and immersed in methanol (B)

After that, the silk fibroin film surface was cross-linked by immersion in a mixture of 0.5 mg/ml 1-ethyl-3-(3-dimethyl aminopropyl) carbodiimide hydrochloride (EDC/HCl) and 0.7 mg/ml N-hydroxysuccinimide (NHS) solution (*Figure 11.A*) in PBS of pH 7.4 at 4°C for 15 minutes to modify the stable water-insoluble surface (*Figure 12*).

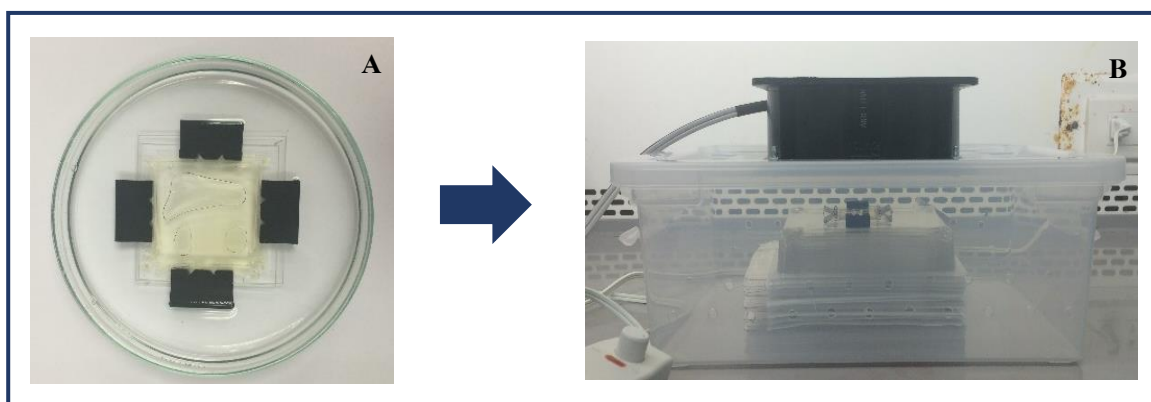


**Figure 11.** Picture of silk fibroin film which was dipped in 1 mg/ml collagen in 0.01 M acetic acid (A) and dry overnight in the chamber with an internal blower (B)

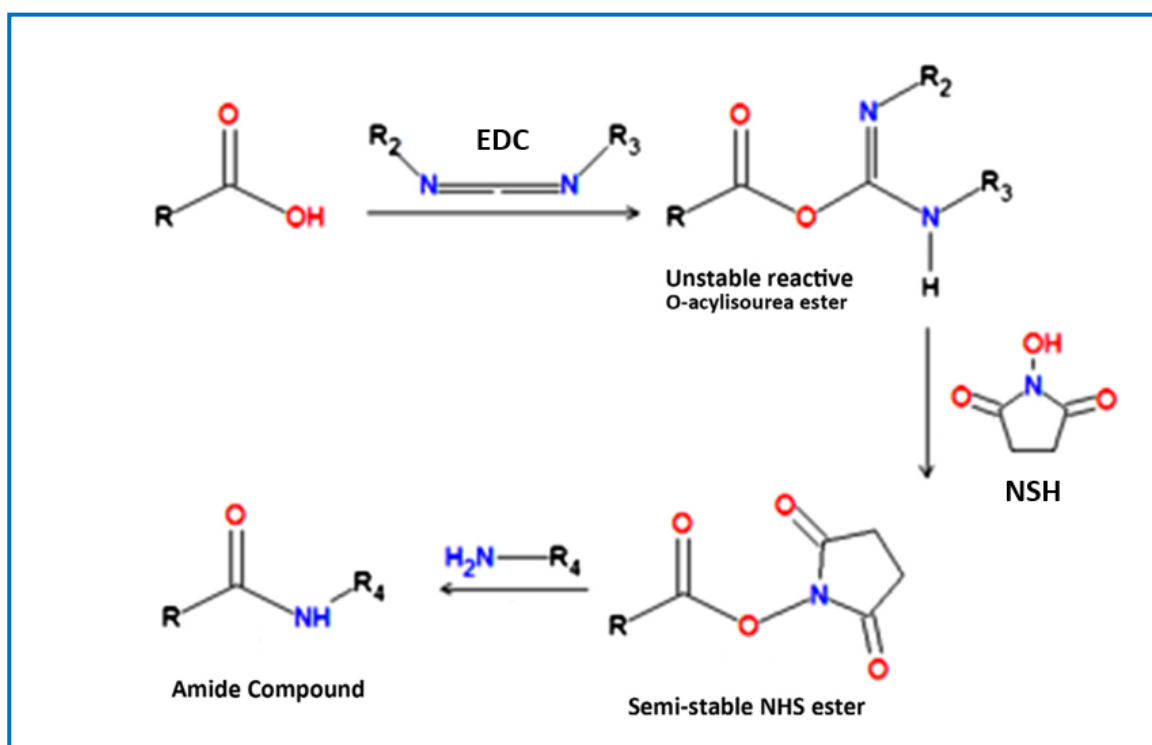


**Figure 12.** The mechanism of 1-ethyl-3-(3-dimethyl aminopropyl) carbodiimide / N-hydroxysuccinimide (EDC/NHS) reaction (57)

The silk fibroin film in group B was soaked with PBS of pH 7.4 at room temperature for 30 minutes. Then, one side of the silk fibroin film surface in group B was dipped in mixture of 1 mg/ml freeze-dried acid-soluble collagen (ASC) which was dissolved in 0.01 M acetic acid at 4 °C and PBS of pH 7.4 at the room temperature in the ratio 1:1 for 12 hours and dried overnight in chamber with an internal blower (Figure 11.B). Measurement of film thickness was performed.

## Phase II: Characterization with physical and mechanical properties

Five samples per group were measured in the experimental study.

### 2.1 Measurement of physical properties

#### 2.1.1 Scanning Electron Microscope (SEM)

The morphological structure and surface roughness of the barrier membranes were observed using SEM at 5-10 kV (FEI Quanta 400, Czech Republic) (Figure 13). The barrier membranes were cut into small pieces, fixed on a metal plate covered with adhesive carbon tape and coated with gold, respectively.

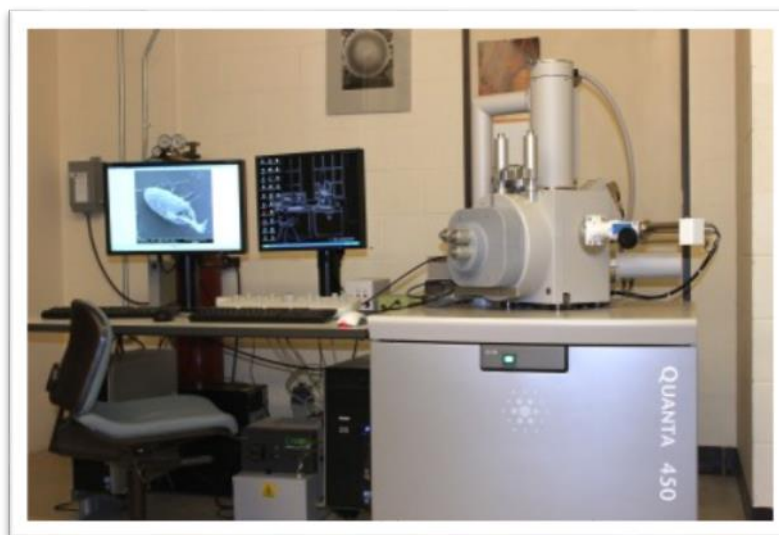


*Figure 13. Photograph of FEI Quanta 400 machine (58)*

#### 2.1.2 Fourier Transform Infrared Spectroscopy (FTIR)

The molecular structural organization of silk fibroin and collagen were characterized using FTIR (Bruker EQUINOX 55, Germany) (Figure 14). The wave numbers ranged from 500 to 4,000  $\text{cm}^{-1}$  using the KBr disc technique with Attenuated Total Reflectance (ATR) mode.



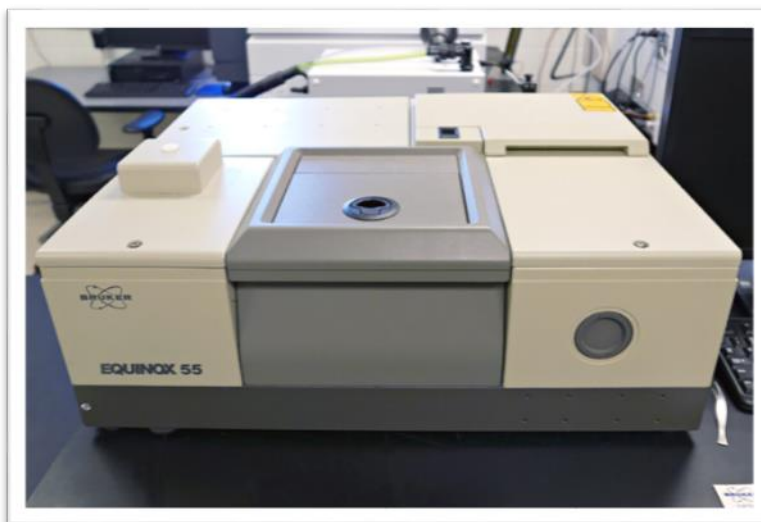


*Figure 14. Photograph of Bruker EQUINOX 55 (59)*

### **2.1.3 Contact angles**

The hydrophilic surfaces or hydrophobic surfaces of the barrier membranes was defined by contact angle meter using the sessile drop technique (OCA 15EC, DataPhysics instrument, Germany) (Figure 15). The sample was fixed on a metal plate before dropping water on the sample surface. Three points of surfaces in different areas were measured to define the angle of the water drop.



*Figure 15. Photograph of OCA 15EC (60)*

### **2.1.4 Atomic Force Microscopy (AFM)**

The surface topography and roughness of the barrier Photo membranes were observed using atomic force microscopy (AFM) (Nanosurf easy scan 2, Nanosurf, Switzerland) (Figure 16) with tapping mode. Images were analyzed by Topography-Scan forward line fit mode.



*Figure 16. Photograph of Nanosurf easy scan 2 (61)*

## 2.2 Measurement of mechanical properties

### 2.2.1 Tensile properties

Five samples per group were measured by observer-blinded to the experimental study. Tensile properties of barrier membranes were performed by a LRXPlus universal testing machine (Lloyd instruments, AMETEK<sup>®</sup> Inc., UK) (*Figure 17.A*).

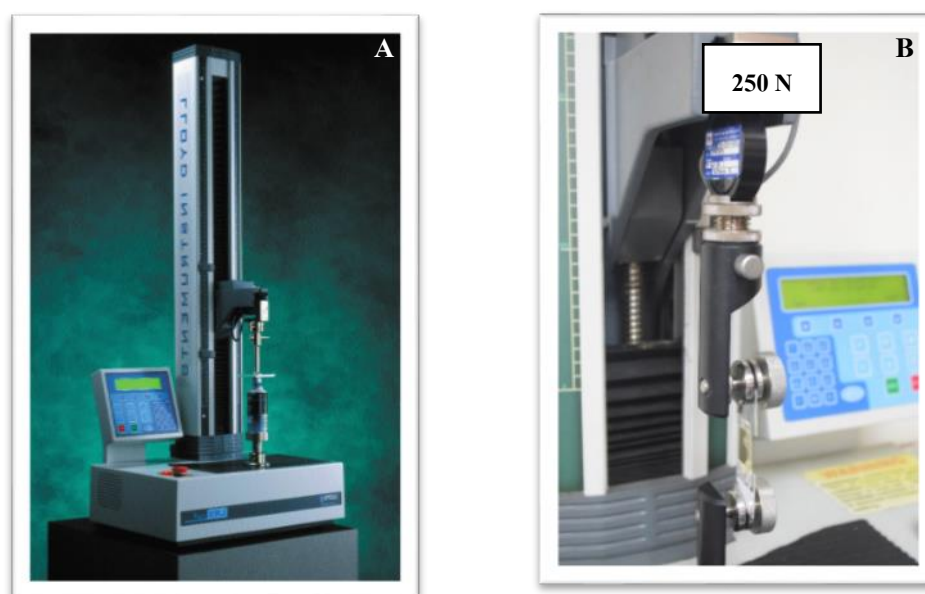


*Figure 17. Photograph of LRXPlus universal testing machine (62)*

The mechanical properties of samples were performed using a tensile strength machine. The barrier membranes were cut into rectangular shapes; size 5 x 30 mm. The samples were immersed in distilled water for 24 hours prior to the mechanical properties examination. Then, the samples were fixed with acrylic jigs at both tails (*Figure 17.B*). The initial length gauge was 20 mm. The tensile force was continuously applied at speed of 10 mm/min and a maximum load-maximum

elongation graph was obtained. The percentage of elongation and stiffness could be measured from this graph. The percentage of elongation of the barrier membranes were determined according to the following *Equation 1*.

$$\text{Percentage of elongation (\%)} = [(L_x - L_0)]/L_0 \times 100$$

**Equation 1.** *Percentage of elongation*

Where  $L_0$  and  $L_x$  denoted the initial gage length of barrier membranes and the maximum elongation of barrier membranes at a predetermined time, respectively.

The mechanical properties of the barrier membranes were performed using a LRXplus series materials testing machine (Ametek<sup>®</sup>, Hampshire, UK). The barrier membranes were cut into rectangular shapes; size 5 mm x 30 mm. The samples were immersed in distilled water for 5 minutes prior to the mechanical properties examination. Then, applied tensile force speed of 10 mm/min. The stress and strain were continuously applied, and a maximum loading-elongation graph was obtained. The tensile strength, percentage of elongation, stiffness, and Young's modulus were measured from this graph.

### 2.2.2 Swelling degree (%)

The samples were cut into size 10 x 10 mm as shown in *Figure 18*. The swelling degree of the barrier membranes was performed after soaking in SBF of pH 7.4 at 37°C for 24 hours. The volume changes of the barrier membranes were recorded at regular time intervals during the course of swelling. The swelling degree of the barrier membranes was determined according to the following *Equation 2*.

$$\text{Swelling Degree (\%)} = [(W_t - W_0)]/W_0 \times 100$$

**Equation 2.** *Swelling degree*

Where  $W_0$  and  $W_t$  denoted the volume of the dry barrier membranes and the volume of the swollen barrier membranes at a predetermined time, respectively.

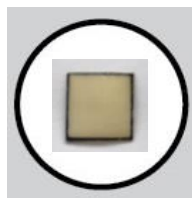


**Figure 18.** *Illustration of sample size 10 x 10 mm*

### 2.2.3 Degradation degree (%)

The degradation degree was performed using lysozyme. The weight of barrier membranes sizes 10 mm x 10 mm (*Figure 18*) were measured and incubated in 4mg/ml lysozyme dissolved in SBF at 37°C. Evaluation of samples at time point 1, 7, 14, 21 and 28 days, the residual samples were removed and dried in a vacuum oven. The initial and final dry weights were used to calculate the percentage of the remaining weight of samples according to the following *Equation 3* (63).

$$\text{Degradation Degree (\%)} = [(W_t - W_0)]/W_0 \times 100$$

*Equation 3.* Degradation degree

Where  $W_0$  and  $W_t$  denoted the initial weight of the barrier membranes and the final weight of the swollen barrier membranes at a predetermined time, respectively.

### Phase III: Biocompatibility testing

Five samples per group were measured in the experimental study.

#### 3.1 Cell culturing of MC3T3-E1 osteoblasts

MC3T3-E1 osteoblasts (ATCC, USA) were cultured in Alpha-Minimum Essential Medium ( $\alpha$ -MEM) supplemented with 10% fetal bovine serum (FBS), 1% penicillin/streptomycin and 0.1% Fungizone (all from Gibco<sup>®</sup>, Invitrogen, USA) in a humidified atmosphere with 5% CO<sub>2</sub> until confluent at 37°C.

#### 3.2 Cell attachment and morphology

The barrier membranes were trimmed in size 10x10 mm and fixed to the bottom of a 24-well plate with a double-sided adhesive tape. Prior to cell seeding, the barrier membranes were soaked in distilled water for 24 hours. Then, distilled water was removed and the cells at a density of  $1 \times 10^4$  cells/cm<sup>2</sup> were seeded on the barrier membrane. The cells were seeded on a 24 well-plate directly as a control group. The cell morphology of MC3T3-E1 cells was observed 6 hours after cell seeding via SEM (64). The barrier membrane was removed from the culture plates, rinsed with PBS and fixed in 2.5% glutaraldehyde (Sigma Aldrich, USA) in PBS for 2 hours. After that, the barrier membrane was dehydrated in an ethanol series of 50 - 100% and coated with gold.

### **3.3 Cell proliferation assay**

The culture period of MC3T3-E1 cells was 14 days. Cell proliferation was measured on days 1, 3, 5 and 7 of the culture periods by using WST-1 assay at 450 nm at each time points (64). The levels of optical density (OD) were used to compare with a standard curve to calculate the amounts of the cells. All culture medium was changed every 3 days.

### **3.4 Cell viability assay**

Fluorescence microscopy was used to assess living cells on the barrier membrane by staining with fluorescein diacetate (FDA, 5 mg/ml acetone). The barrier membrane was removed from the culture medium and rinse with PBS 3 times. The 1 ml of medium and 5  $\mu$ l of FDA was added to each barrier membrane respectively and kept in the dark at 37 °C for 5 min. Then, the barrier membrane was rinsed with PBS 3 times and observed by the fluorescence microscopy(65).

### **3.5 Mineralization assay**

Mineralization assay was measured by Alizarin Red S staining on days 14, 21 and 28 of the culture periods.

**Table 6.** Measurement variables

<b>Physical properties and mechanical properties</b>	<b>Operations</b>	<b>Indicators</b>	<b>Scale of measurement</b>
<b>1. Physical properties</b>	<ul style="list-style-type: none"> <li>- Fourier transform infrared spectroscopy (FTIR)</li> <li>- Scanning electron microscopy (SEM)</li> <li>- Contact angles</li> <li>- Atomic force microscopy (AFM)</li> </ul>	<ul style="list-style-type: none"> <li>- Absorbance-wavenumber</li> <li>- Morphology</li> <li>- Contact angles</li> <li>- Surface topography</li> <li>- Surface roughness</li> </ul>	<ul style="list-style-type: none"> <li>Interval</li> <li>Nominal</li> <li>Ratio</li> <li>Nominal</li> <li>Ratio</li> </ul>
<b>2. Mechanical properties</b>	<ul style="list-style-type: none"> <li>- Stress-strain pattern</li> <li>- Degradation over time</li> <li>- Swelling rate</li> </ul>	<ul style="list-style-type: none"> <li>- Percentage of elongation</li> <li>- Stiffness</li> <li>- Degradation degree</li> <li>- Swelling degree</li> </ul>	<ul style="list-style-type: none"> <li>Ratio</li> <li>Ratio</li> <li>Ratio</li> <li>Ratio</li> </ul>
<b>3. Biocompatibility properties</b>	<ul style="list-style-type: none"> <li>- Scanning electron microscopy (SEM)</li> <li>- WST-1 assay</li> <li>- Fluorescence microscopy</li> <li>- Alizarin Red S staining</li> </ul>	<ul style="list-style-type: none"> <li>- Cell attachment morphology</li> <li>- Cell proliferation</li> <li>- Cell viability</li> <li>- Mineralization</li> </ul>	<ul style="list-style-type: none"> <li>Nominal</li> <li>Ratio</li> <li>Nominal</li> <li>Ratio</li> </ul>

### **Statistical analysis**

The statistical analysis was performed using SPSS software (Version 16.0, SPSS Inc., Chicago, IL, USA). An analysis of variance (ANOVA) was used to compare experimental groups. The statistical significance was defined as P-value less than 0.05.

## CHAPTER 3

### RESULTS

#### Morphology

The silk fibroin film in group A and the silk fibroin-collagen in group B had transparent cloudy yellow color and showed no porosity on both sides. The silk fibroin film in group A had a non-homogeneous texture surface on one side (*Figure 19.A*), while the other side had a smooth surface (*Figure 19.B*). The silk fibroin-collagen in group B also had a non-homogeneous texture surface on one side (*Figure 20.C*), while the other side had a smooth surface (*Figure 20.D*). But, the silk fibroin film in group A was softer and less bending than the silk fibroin-collagen film in group B. While, the surfaces of commercial collagen membrane (Bio-Gide<sup>®</sup>) in group C were different. One side had a rough surface with some fibers (*Figure 21.E*) when the other side had a dense smoother surface (*Figure 21.F*).

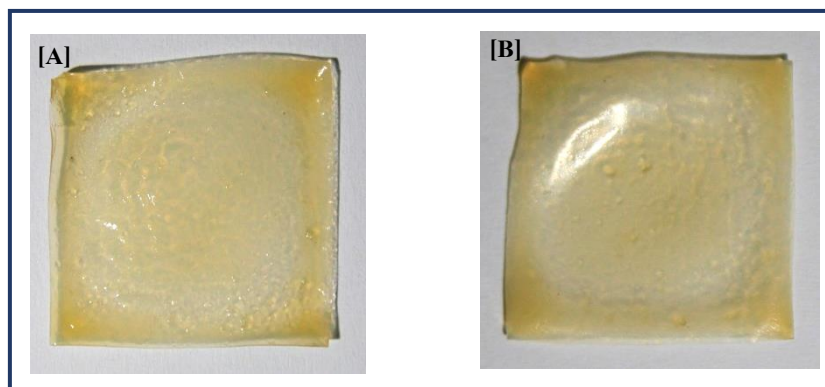


**Figure 19.** Pictures of front side (A) and back side (B) of the silk fibroin film; size 30 x 30 mm

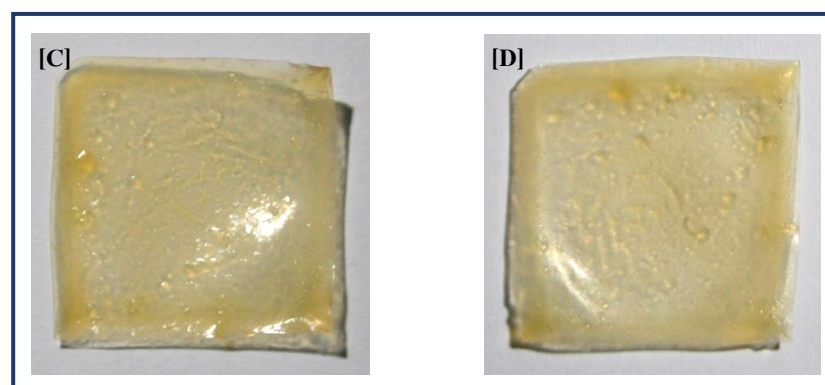


**Figure 20.** Pictures of front side (C) and back side (D) of the silk fibroin-collagen film;  
size 30 x 30 mm

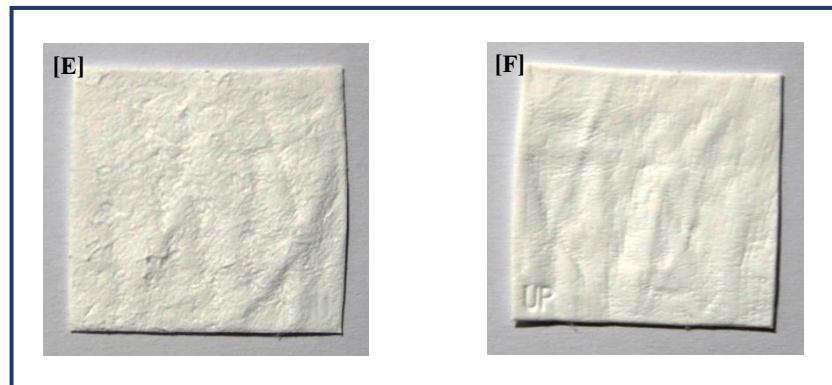


**Figure 21.** Pictures of fibrous surface (E) and dense surface (F) of commercial collagen membrane (Bio-Gide®); size 35 x 35 mm

The thickness of the samples was shown in Figure 22. The silk fibroin film in group A (SG) had average thickness  $0.338 \pm 0.01$  mm more than the silk fibroin-collagen film (SG-Col) ( $0.299 \pm 0.10$  mm) and less than the commercial collagen membrane (Collagen) ( $0.532 \pm 0.05$  mm). The commercial collagen membrane showed the highest thickness significant difference from the other groups.

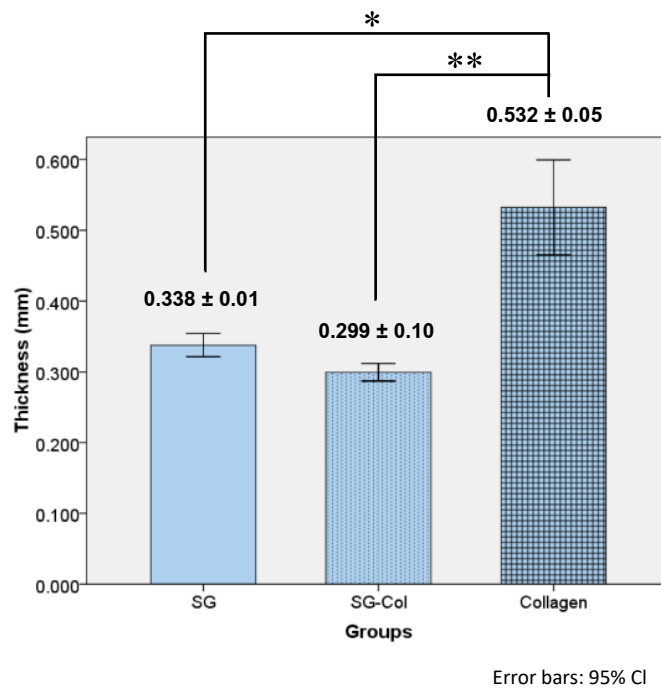


**Figure 22.** Mean thickness of silk fibroin film (SG), silk fibroin-collagen film (SG-Col) and commercial collagen membrane (Bio-Gide®)



### Scanning Electron Microscope (SEM)

The SEM examination demonstrated a rough surface without porosity on both sides of the silk fibroin film (*Figure 23.A, B*). The silk fibroin-collagen film had a rougher surface with collagen organized into a fibril structure covering on one surface (*Figure 23.C*), which was differed from another side that showed no porosity surface (*Figure 23.D*) which was the same as both surfaces of silk fibroin film. The commercial collagen membrane demonstrated loose collagen fibril organization (*Figure 23.E*) while the outer surface showed the dense collagen fibril surface (*Figure 23.F*).

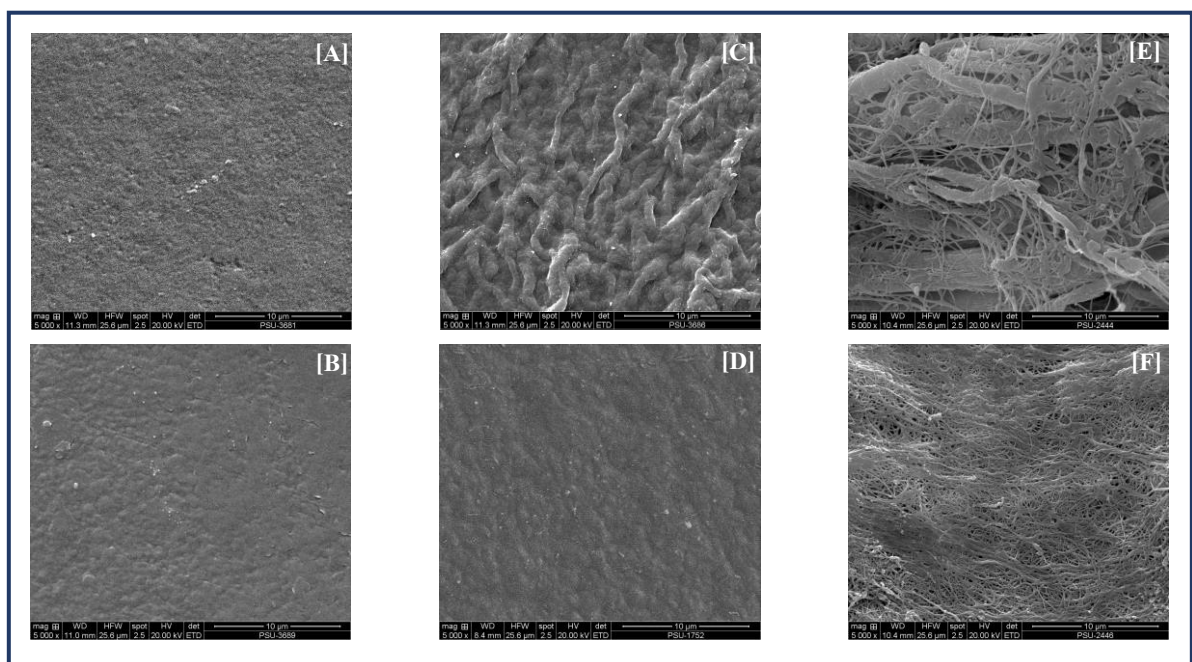


**Figure 23.** SEM photograph of the front side and back side of silk fibroin film (A, B), silk fibroin-collagen film (C, D) and commercial collagen membrane (Bio-Gide®) (E, F)  
Magnification x 5,000

### Atomic Force Microscopy (AFM)

Surface topography was characterized by Atomic Force Microscopy (AFM). Surfaces of both fabricated experiment groups showed a rough surface. The top surface of the silk fibroin-collagen film showed the highest rough among study groups (*Figure 25.C*).

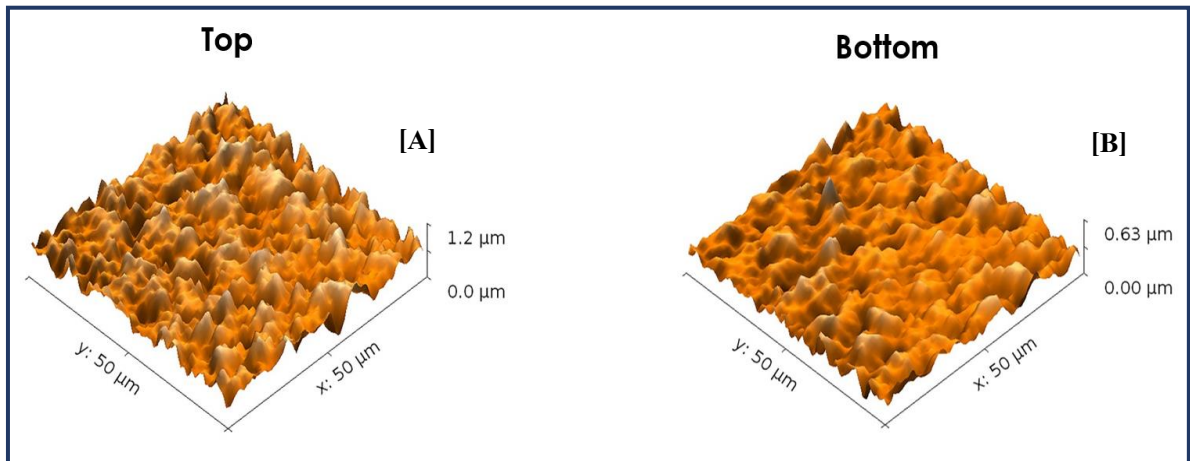


**Figure 24.** The 3D of AFM photograph of the front side (A) and back side (B) of silk fibroin film

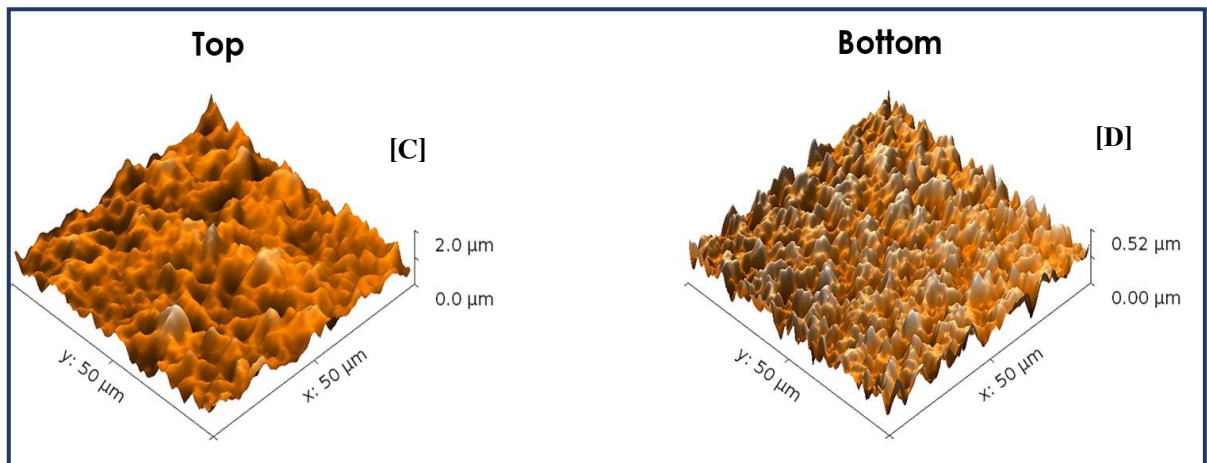


**Figure 25.** The 3D of AFM photograph of the front side (C) and back side (D) of silk fibroin-collagen film

### Surface roughness

RMS was representations of surface roughness which was calculated as the Root Mean Square of a surface measured microscopic peaks and valleys (Equation 4). Assessment of RMS value founded that the top surface of silk fibroin film and silk fibroin-collagen film had 0.1424 and 0.2155  $\mu\text{m}$ , respectively. While, the bottom surface of silk fibroin film and silk fibroin-collagen film had 0.0660 and 0.0699  $\mu\text{m}$ , respectively (Table 7). RMS values of the top surface of silk fibroin-collagen film showed higher values when compared with silk fibroin film because of collagen immobilization on the surface of silk fibroin which made the surface of silk fibroin-collagen film had higher surface roughness when characterized by Atomic Force Microscopy (AFM). On the other hand, RMS values of the bottom surface of the silk fibroin-collagen film showed a little higher value when compared with silk fibroin film.

$$\text{RMS} = \sqrt{\frac{1}{n} \sum_{i=1}^n y_i^2}$$

**Equation 4.** Root Mean Square of a surface

**Table 7.** The surface roughness (RMS) of barrier membranes

Groups	Top ( $\mu\text{m}$ )	Bottom ( $\mu\text{m}$ )
Silk fibroin film in group A	0.1424	0.0660
Silk fibroin-collagen film in group B	0.2155	0.0699
Commercial collagen membrane in group C	-	-

#### Fourier Transform Infrared Spectroscopy (FTIR)

The molecular structural formation of samples was characterized by FTIR using the KBr disc technique with Attenuated Total Reflection (ATR) mode. The wave numbers ranged from 500 to 4,000  $\text{cm}^{-1}$ . The position of wavenumber peak of the silk fibroin-collagen film (SG) (green line), the silk fibroin-collagen film (SG-Col) (Blue line) and commercial collagen membrane (Bio-Gide<sup>®</sup>) (Collagen) (light blue line) from FTIR were shown in *Figure 26*.

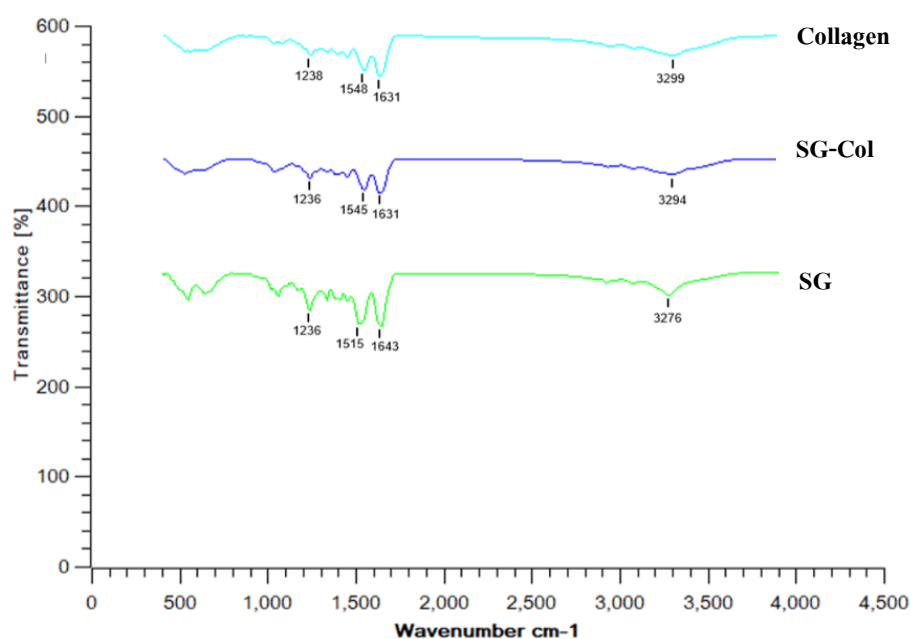


**Figure 26.** The infrared absorption spectrum of silk fibroin-collagen film (Green line), silk fibroin-collagen film (Blue line) and commercial collagen membrane (Bio-Gide<sup>®</sup>) (Light blue line)

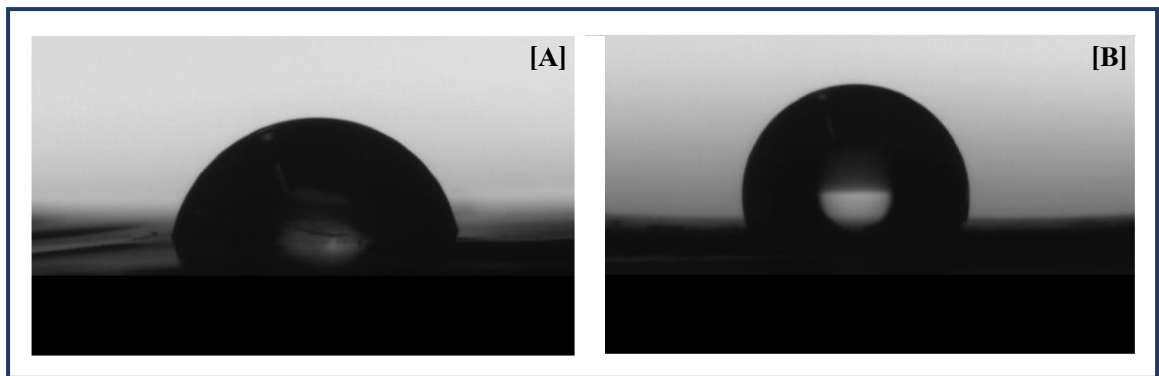
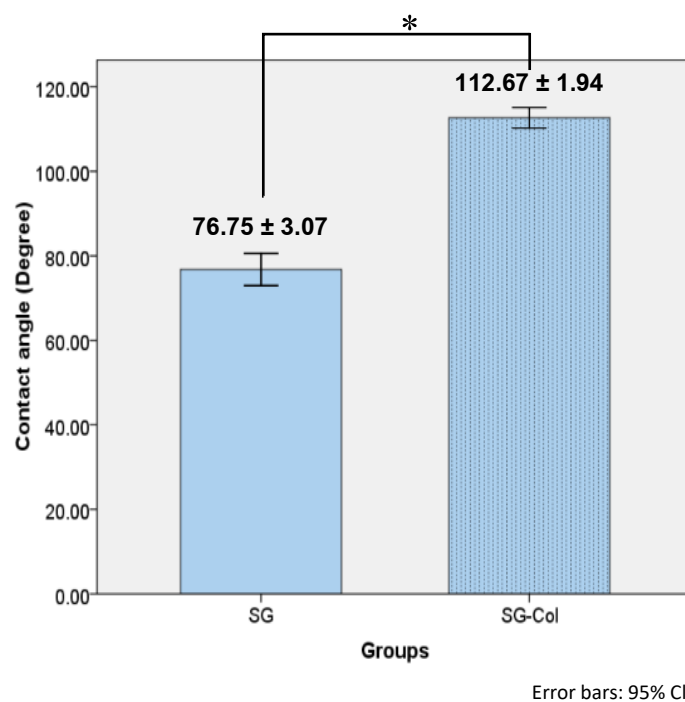
The infrared absorption spectrum of proteins was dominated by the absorption of the peptide bonds; amide I peak of the silk fibroin-collagen film and commercial collagen membrane was found at the same peak which was at  $1,631\text{ cm}^{-1}$  while the silk fibroin film was found at  $1,643\text{ cm}^{-1}$ . Amide II peak of the silk fibroin film was found at  $1,515\text{ cm}^{-1}$  which were lower wavenumber when compared with the silk fibroin-collagen film in group B ( $1,545\text{ cm}^{-1}$ ). Moreover, Amide II peak of the silk fibroin-collagen film was similar when compared with commercial collagen membrane which was found at  $1,548\text{ cm}^{-1}$ . Amide III peak of the silk fibroin film and the silk fibroin-collagen film were found at the same peak which was at  $1,236\text{ cm}^{-1}$ . Amide III peak of commercial collagen membrane was found at  $1,238\text{ cm}^{-1}$ . Amide A peak of the silk fibroin film, the silk fibroin-collagen film, and commercial collagen membrane were found at  $3276$ ,  $3294$  and  $3299\text{ cm}^{-1}$ , respectively. Comparison between the silk fibroin film and the silk fibroin-collagen film demonstrated that the position of amide I peak was shifted to higher wavenumber. The position of amide II peak was shifted to lower wavenumber. While the position of amide III peak and amide A peak in both fabricated experimental groups had the same point.

### **Contact angle ( $^{\circ}$ ) analysis**

The hydrophobic-hydrophilic surface of the silk fibroin film (SG), the silk fibroin-collagen film (SG-Col) and commercial collagen membrane (Bio-Gide<sup>®</sup>) was assessed by water contact angle test and was shown in *Table 8*. A silk fibroin film had an average contact angle as  $76.75^{\circ} \pm 3.07$  (*Figure 27.A*) which was lower than the average contact angle of the silk fibroin-collagen film ( $112.67^{\circ} \pm 1.94$ ) (*Figure 27.B*) significantly (P-values  $< 0.05$ ). The hydrophilic surface showed a contact angle of more than  $90^{\circ}$  and the hydrophobic surface showed a contact angle of less than  $90^{\circ}$ . This measurement was reported that the silk fibroin-collagen film caused more obtuse contact angle which indicated a hydrophobic surface. The commercial collagen membrane could not be measured by this method due to the membrane easily absorbed water.

**Table 8.** The contact angle of samples

	Contact angle (°)	
	SG	SG-Col
1	78.75	111.30
2	79.66	112.79
3	71.77	110.22
4	77.25	114.01
5	76.34	115.01
Average	76.75° ± 3.07	112.67° ± 1.94

**Figure 27.** Pictures of silk fibroin film (A) and silk fibroin-collagen film (B)**Figure 28.** Mean contact angle of silk fibroin film (SG) and silk fibroin-collagen film (SG-Col)

\*Significantly difference strongly from silk fibroin group at  $P$ -value < 0.05

## Mechanical properties

### Percentage of elongation (%)

Ductility of barrier membrane could be explained by the percentage of elongation. The *Table 9* and *Figure 29* showed a comparison between study groups and the percentage of elongation. The average percentage of elongation of the silk fibroin film (SG;  $28.93 \pm 15.56$ ) was less than the silk fibroin-collagen film (SG-Col;  $42.10 \pm 11.46$ ) and Bio-Gide<sup>®</sup> collagen membrane (Collagen;  $54.79 \pm 13.44$ ) but still had elongation property at around 29 percent. The results showed no significant difference among study groups ( $P\text{-value} > 0.05$ )

**Table 9.** Maximum elongation and percentage of elongation of experimental groups

	Silk fibroin film in group A		Silk fibroin-collagen film in group B		Collagen membrane in group C	
	Maximum elongation (mm)	Percentage of elongation (%)	Maximum elongation (mm)	Percentage of elongation (%)	Maximum elongation (mm)	Percentage of elongation (%)
<b>1</b>	10.43	52.15	10.05	50.25	13.08	65.40
<b>2</b>	4.40	22.00	10.61	53.05	7.53	37.65
<b>3</b>	3.79	18.92	7.22	36.10	10.10	50.50
<b>4</b>	4.52	22.61	5.80	29.00	13.12	65.60
<b>Average</b>		<b><math>28.93 \pm 15.56</math></b>		<b><math>42.10 \pm 11.46</math></b>		<b><math>54.79 \pm 13.44</math></b>

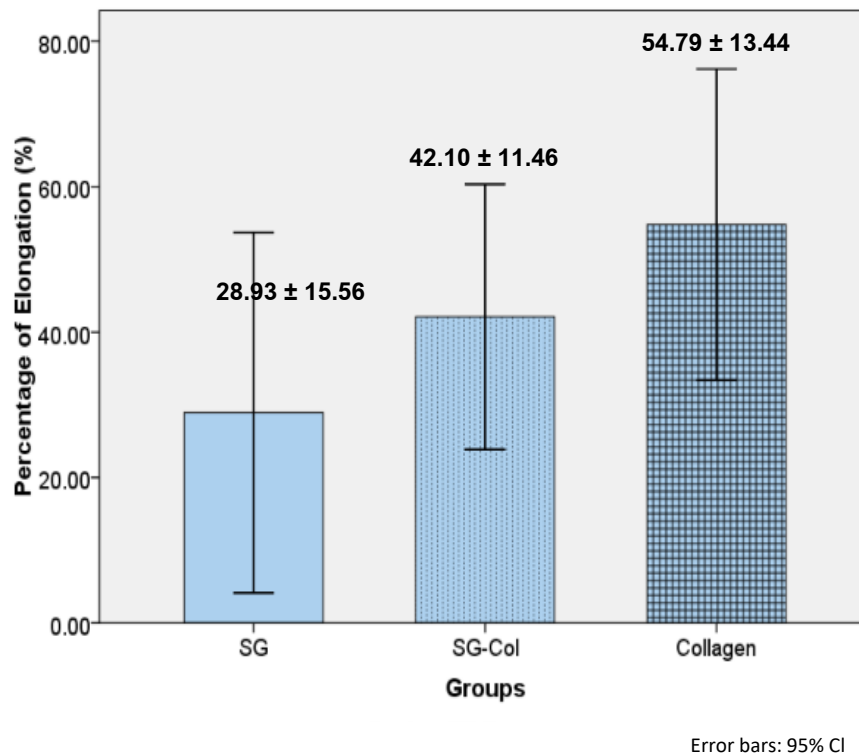


**Figure 29.** Mean percentage of elongation of silk fibroin film (SG), silk fibroin-collagen film (SG-Col) and commercial collagen membrane (Bio-Gide®)

#### Stiffness or Modulus of Elasticity

Stiffness is the rigidity of sample which resists deformity of an object when applied force. Average stiffness of the silk fibroin-collagen film (SG-Col;  $2,485.7 \pm 555.8$ ) was the highest and showed both statistically significant difference from the silk fibroin film (SG;  $1,758.0 \pm 317.0$ ) and commercial collagen membrane (Bio-Gide®) (Collagen;  $1,101.0 \pm 463.8$ ) as shown in Table 10 and Figure 30. High stiffness referred to the less flexible of the barrier membrane.

**Table 10.** The stiffness of experimental groups

Group	Stiffness (N/m)
Silk fibroin film in group A	$1,758.0 \pm 317.0$
The silk fibroin-collagen film in group B	$2,485.7 \pm 555.8$
Commercial collagen membrane (Bio-Gide®) in group C	$1,101.0 \pm 463.8$

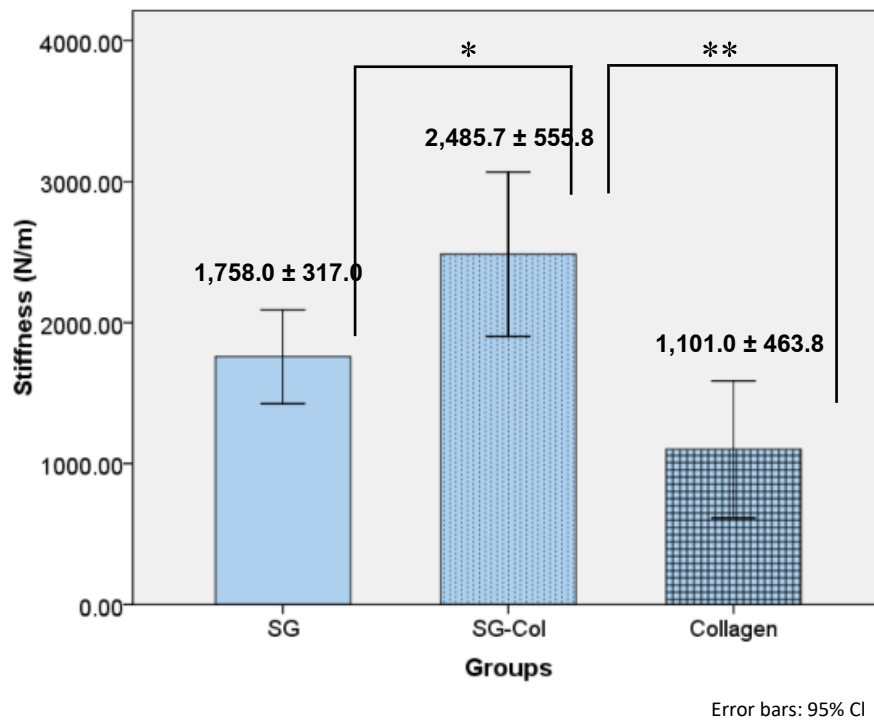


**Figure 30.** Mean stiffness of silk fibroin film (SG), silk fibroin-collagen film (SG-Col) and commercial collagen membrane \*Significantly higher than SG, \*\*Significantly higher than collagen

### Swelling degree

The results of the swelling degree of samples in SBF of pH 7.4 at 37°C over time was shown in *Table 11*. The swelling degree was increased with time and tended to be stable after soaking in SBF for one hour in all study groups. The results clearly indicated that commercial collagen membrane exhibited the maximum swelling degree and much more than other groups significantly (P-value < 0.05) (*Figure 31*).

**Table 11.** Swelling degree of experimental groups

Time	Swelling degree (wt%)		
	SG	SG-Col	Collagen
5 minutes	61.31 ± 4.09	69.35 ± 1.33	486.74 ± 34.67
15 minutes	85.92 ± 3.36	107.01 ± 1.37	509.12 ± 27.64
30 minutes	106.46 ± 3.44	115.31 ± 1.55	528.16 ± 25.08
1 hour	109.47 ± 3.79	122.20 ± 2.85	530.74 ± 25.97
6 hours	110.25 ± 3.75	123.36 ± 3.04	532.38 ± 25.56
12 hours	111.15 ± 3.65	123.71 ± 2.82	532.64 ± 25.91
24 hours	111.26 ± 3.51	124.19 ± 2.71	533.24 ± 25.67



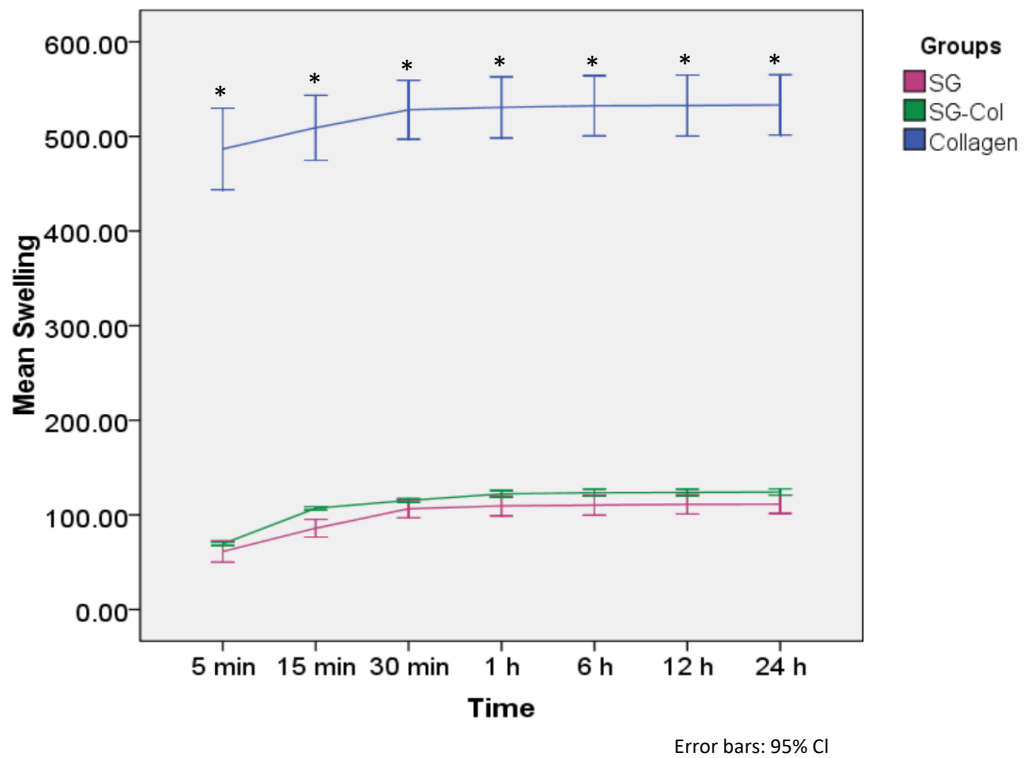


**Figure 31.** Mean swelling degree of silk fibroin film (SG), silk fibroin-collagen film (SG-Col) and commercial collagen membrane (Bio-Gide®) \*Significantly higher than other groups within the same time

### Degradation degree

The degradation degree was assessed to investigate the degradation of the silk fibroin film (SG), the silk fibroin-collagen film (SG-Col) and commercial collagen membrane (Collagen) according to the method. *Table 12* showed the degradation degree of samples which were incubated in lysozyme dissolved in SBF at 37°C over time. At Day 1, there was no significant difference among study groups. On Day 7 and 14, the commercial collagen membrane had slower degradation than other groups and showed a significant difference (P-value < 0.05) when compared with silk fibroin film and silk fibroin-collagen film. At Day 21 and 28, the degradation degree in silk fibroin-collagen groups was higher than other groups significantly (P-value < 0.05) (*Figure 32*).

**Table 12.** Degradation degree of experimental groups

Day	Degradation degree (wt%)		
	SG	SG-Col	Collagen
Day 1	3.41 ± 0.70	2.44 ± 0.23	1.68 ± 0.30
Day 7	7.01 ± 1.10	9.79 ± 1.79	4.34 ± 0.54
Day 14	13.41 ± 1.51	17.76 ± 2.01	6.95 ± 0.50
Day 21	17.17 ± 4.68	22.20 ± 5.41	11.79 ± 4.07
Day 28	20.94 ± 5.22	29.30 ± 6.97	16.35 ± 4.89

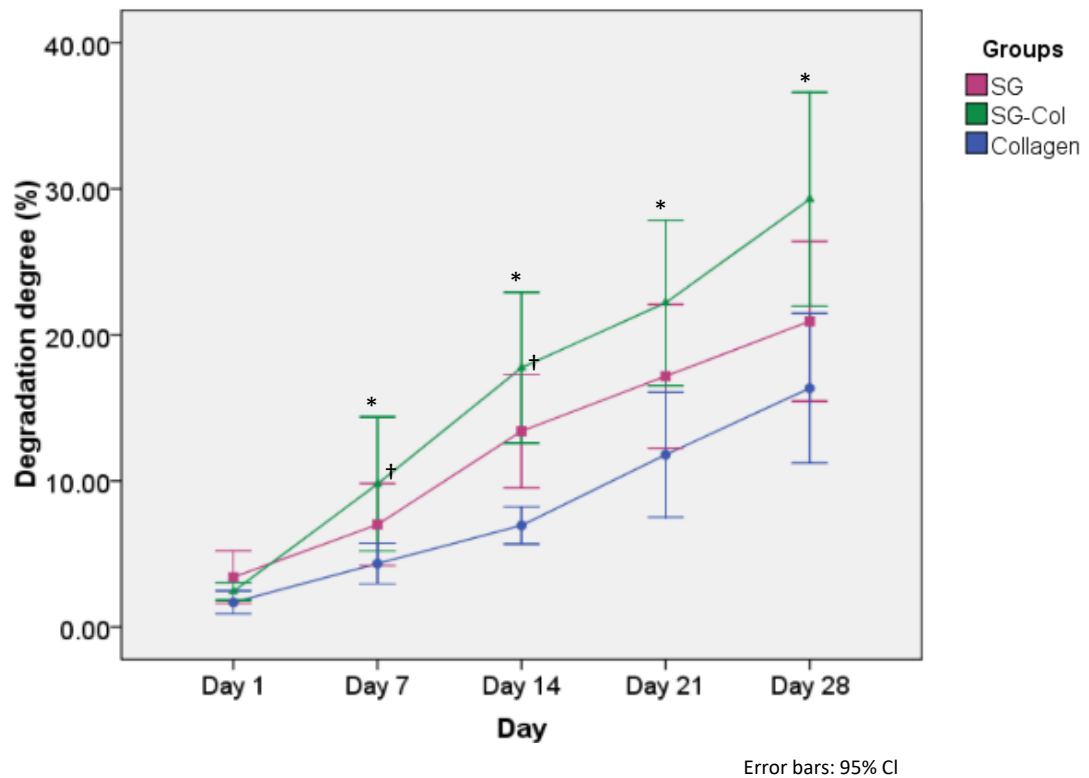


**Figure 32.** Mean degradation degree of silk fibroin film (SG), silk fibroin-collagen film (SG-Col) and commercial collagen membrane (Bio-Gide®) \*Significantly higher than other groups within the same time, † Significantly higher than the only collagen within the same time

## Cell attachment

The cell morphology of MC3T3-E1 cells was observed 6 hours after cell seeding via SEM and shown in *Figure 33*. The SEM examination revealed different osteoblasts morphology among study groups. Osteoblast-like cells adhered on silk fibroin film and commercial collagen membrane in a spindle-shape and had elongated filopodia (*Figure 33.A, E*) Moreover, commercial collagen membrane had multiple extending filopodia, but membrane was contaminated with some residual chemical particles onto the collagen fibrils (*Figure 33.F*). Most of osteoblasts cell which attached on silk fibroin-collagen film were in round-shape or polygonal without filopodia (*Figure 33.D*).

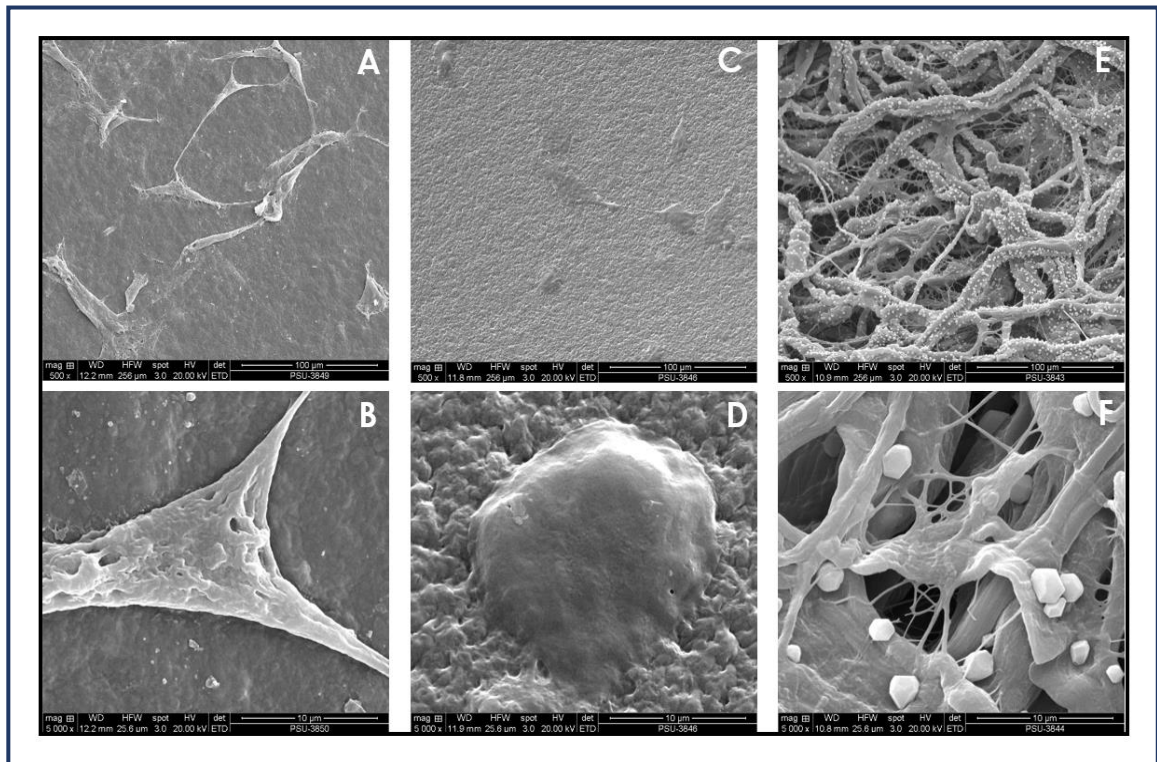


**Figure 33.** The SEM photograph of cell morphology attached to silk fibroin film in group A (A, B), the silk fibroin-collagen film in group B (C, D), and commercial collagen membrane (Bio Gide®) in group C (E, F)

### Cell viability assay

The results of fluorescence microscopy images showed living cells attachment were widely distributed on the surface of the samples as shown in *Figure 34*. The density of viable cells predominantly increased with time, which indicates that the membrane had the ability to maintain cell viability and proliferation.

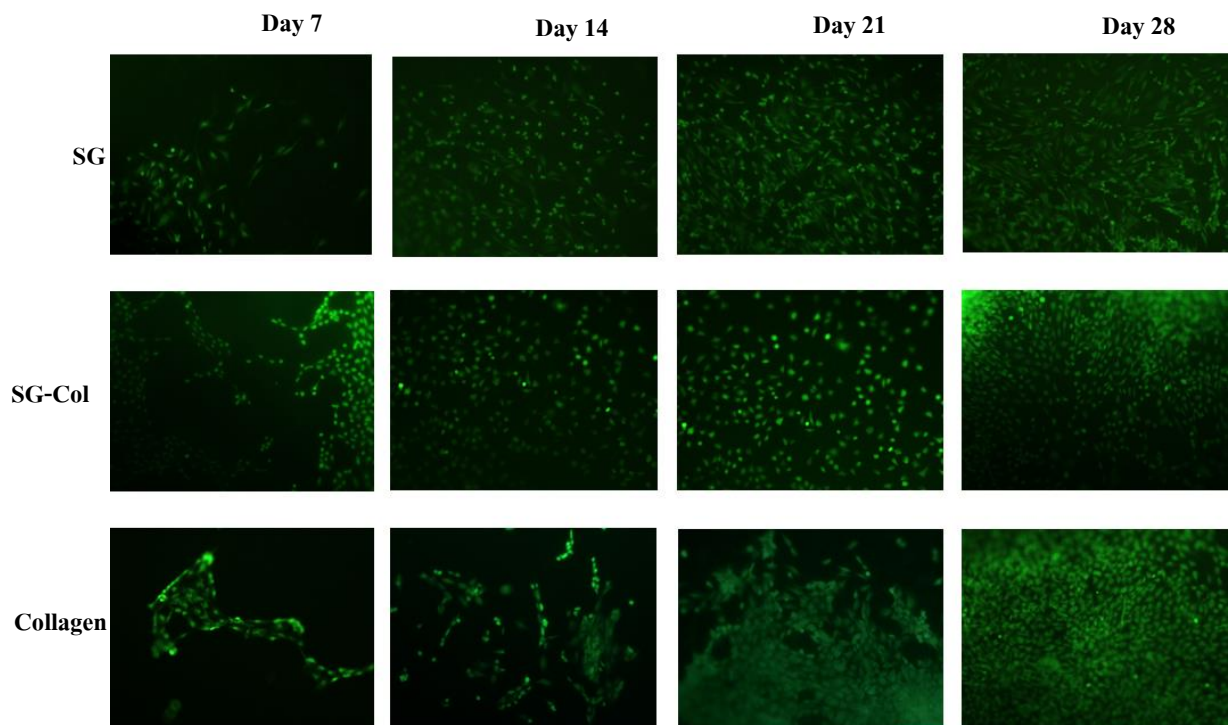


**Figure 34.** Pictures of cell viability of osteoblasts on silk fibroin film, the silk fibroin-collagen film, and commercial collagen membrane (Bio-Gide<sup>®</sup>) (green luminance, FDA labeled)

### Cell proliferation assay

The culture period for MC3T3-E1 cells was 7 days and measurement of cell proliferation of MC3T3-E1 cells was assessed by WST-1 assay on days 1, 3, 5 and 7 of the culture periods. The results of cell proliferation numbers were shown in *Table 13*. All study groups showed a similar pattern of cell proliferation that continuously increased with time in all groups. On culture Day 1 and Day 7, the results showed a significant difference among study groups (P-value < 0.05). On culture Day 3 and Day 5, the silk fibroin film had significantly highest cell numbers significantly (P-value < 0.05). Moreover, the silk fibroin film showed higher cell proliferation than the others at all time points as shown in *Figure 35*. Whereas silk fibroin-collagen film showed the trend similar to commercial collagen membrane and showed no significant difference between groups (P-value > 0.05).

**Table 13.** Cell proliferation numbers of experimental groups

Day	Cell proliferation number (cells)		
	SG	SG-Col	Collagen
Day 1	6,767.50 ± 697.67	1,286.25 ± 511.05	3,900.83 ± 1,046.14
Day 3	6,555.00 ± 858.30	2,505.42 ± 433.33	1,958.58 ± 1,029.62
Day 5	23,213.33 ± 3,542.58	5,380.00 ± 2,626.63	5,488.33 ± 151.18
Day 7	36,784.17 ± 2,681.73	15,905.00 ± 2,148.88	12,317.50 ± 1,267.68

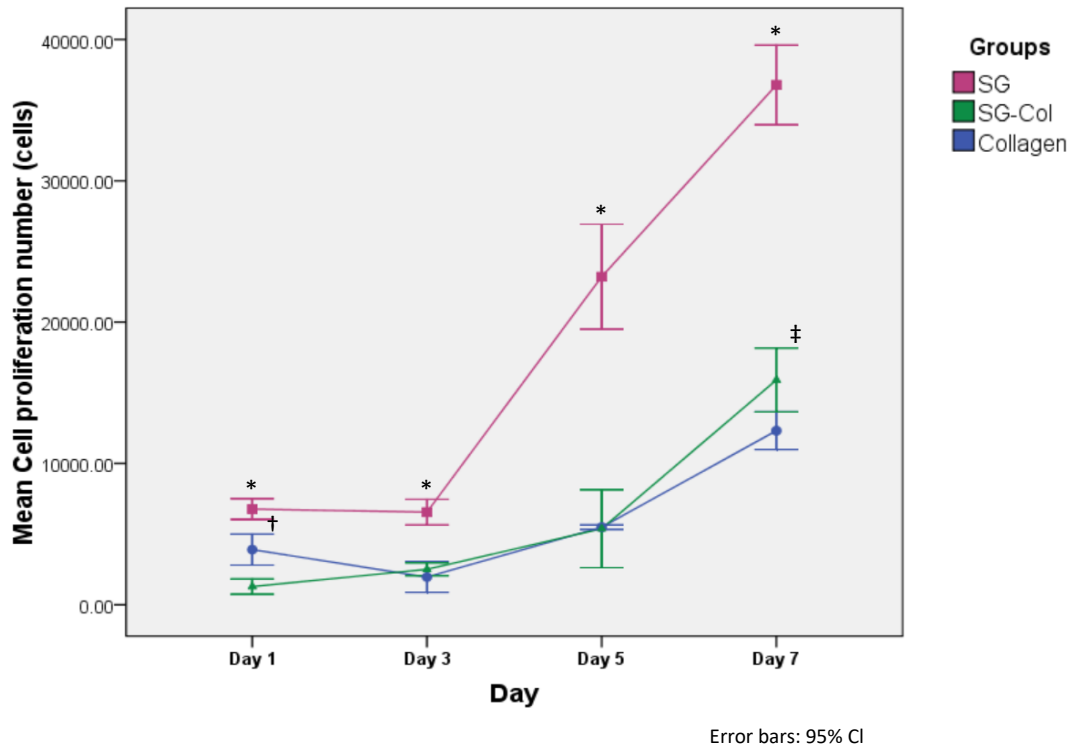


**Figure 35.** Mean cell proliferation numbers of silk fibroin film (SG), silk fibroin-collagen film (SG-Col) and commercial collagen membrane (Bio-Gide®) \*Significantly higher than other groups at the same time, † Significantly higher than only SG-Col at the same time, ‡Significantly higher than the only Collagen within the same time

### Cell mineralization

Mineralization assay was measured by Alizarin Red S staining on days 14, 21 and 28 of the culture periods. The results of optical density (OD) of silk fibroin film, silk fibroin-collagen film, and commercial collagen membrane were shown in *Table 14*. On culture Day 14, both silk fibroin film and commercial collagen membrane showed higher OD when compared with silk fibroin-collagen film and showed a significant difference (P-value < 0.05). But, the comparison between silk fibroin film and commercial collagen membrane showed no significant difference. On culture Day 21, commercial collagen membrane had higher OD than other groups and showed a significant difference (P-value < 0.05). But on culture Day 28, the results showed no significant difference among study groups (P-value > 0.05) *Figure 36*.

**Table 14.** Optical density (OD) of experimental groups

Day	Optical density (OD)		
	SG	SG-Col	Collagen
Day 14	0.56 ± 0.16	0.24 ± 0.07	0.64 ± 0.07
Day 21	0.61 ± 0.05	0.53 ± 0.04	0.98 ± 0.15
Day 28	0.77 ± 0.13	0.56 ± 0.04	0.78 ± 0.19

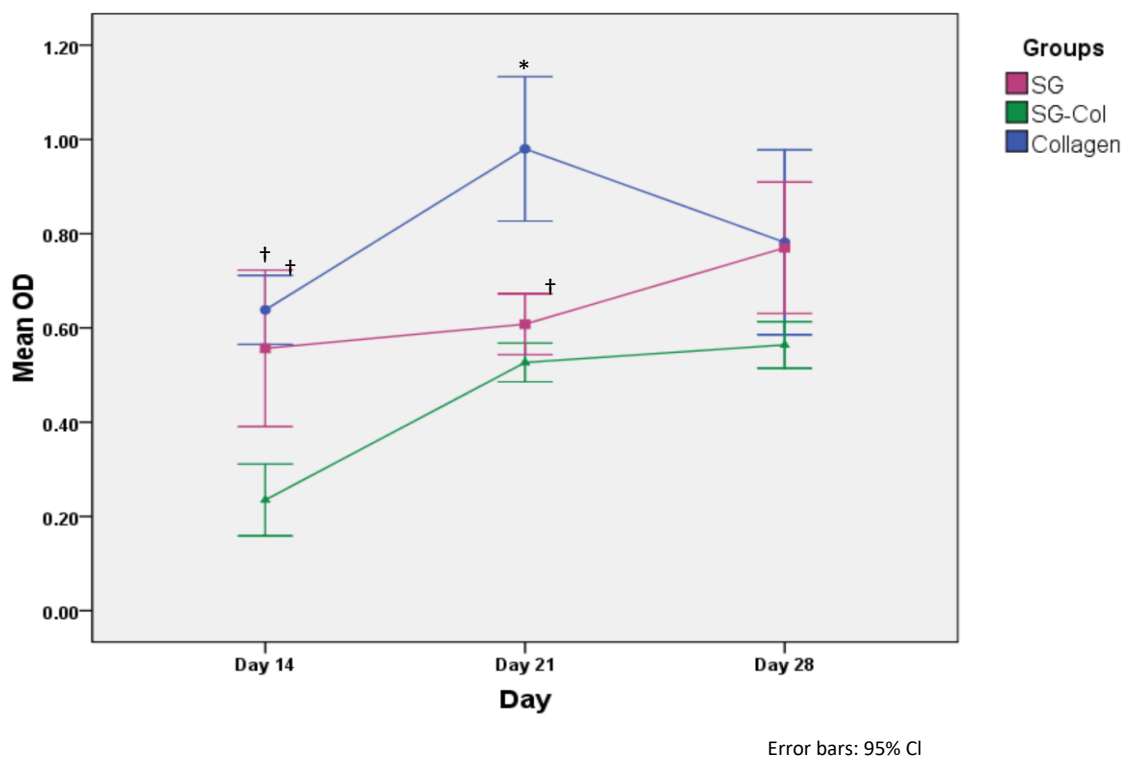


**Figure 36.** Mean optical density of silk fibroin film (SG), silk fibroin-collagen film (SG-Col) and commercial collagen membrane (Bio-Gide®) \*Significantly higher than other groups within the same time, †Significantly higher than only SG-Col within the same time

## CHAPTER 4

### DISCUSSION

This study has fabricated a natural barrier membrane derived from silk fibroin and fish collagen. This new barrier membrane could be kept at room temperature and can be softened after soaking with distilled water, easy to use and can be trimmed to adapt the defects. The barrier membrane was fabricated with the simple materials without antigenic proteins, which was confirmed by Fourier transforms infrared (FTIR) spectroscopy. The FTIR spectrum of a protein was composed of many vibrational bands arising from different functional groups such as N, H, C and O. Major absorption bands of collagens were in the amide band region. The amide I band of a protein depends on the structure of the protein such as  $\alpha$ -helices,  $\beta$ -sheet and random coil structures (66). The amide I, the region of 1620–1680  $\text{cm}^{-1}$ , was primarily due to the amide C=O stretching vibrations and characterized band of  $\beta$ -sheet formation, while N-H bending vibration coupled with C-N stretching vibration found in the region of 1,520– 1,560  $\text{cm}^{-1}$  and formed the amide II band. The amide III bands, were found near the region of 1240  $\text{cm}^{-1}$ , represented N–H bending vibrations and C–H stretching, while the absorption band of 700  $\text{cm}^{-1}$  represented amide IV which was amide group of sericin. The amide A band of collagen which was associated with the N-H stretching was usually found in the region of 3293–3306  $\text{cm}^{-1}$  (67, 68). The peak of amide IV was not found in this study proving that sericin which was antigenic protein was completely removed. Moreover, cell viability results showed osteoblast cells were attached and widely distributed on the surface of the samples which indicated that both silk fibroin film and silk fibroin-collagen film were non-toxic materials. The fabricated membrane could be used for covering small bone defects such as extraction socket, periodontal defect, and peri-implant defect.

The silk fibroin-collagen film showed higher stiffness than the commercial collagen membrane which referred to higher rigidity and less collapse than the commercial collagen membrane. Membrane rigidity was a desirable property of a barrier membrane for providing space maintenance which correlated to potential regenerated bone volume beneath a membrane. The membrane should have adequate stiffness to create and maintain a suitable space for the new bone formation. Besides membrane rigidity, also provide space maintenance the use of particulate grafts, block grafts, tenting screws, and dental implants. A previous study reported on twelve patients who underwent alveolar ridge augmentation using titanium mini-screws for supporting the e-PTFE



membrane for later dental implant placement (31). Following a healing period of six to ten months, the authors demonstrated an increase in new bone formation ranged from 1.5 to 5.5 mm. On the other hand, collagen membrane had lower stiffness and higher water absorption that might not be able to maintain the space. The results agree with Marouf HA et al. that collagen membranes had poor space maintaining ability because of their low rigidity and fast degradation rate (69). Currently, there was no available collagen-based membrane with enough structural rigidity for maintaining shape over the bone defect.

The present study showed that the commercial collagen membrane exhibited five times swelling degree more than other groups. According to Song JH et al. indicated that pure collagen membrane had 130% swelling degree which was too high for use as a barrier membrane for guided bone regeneration (70). In this study, both silk fibroin and silk fibroin-collagen had approximately 100% swelling degree which less than the commercial collagen membrane inferred that they were better in maintaining their form but still had the ability to absorb fluid and allow it to pass through. Moreover, Yun-Jin Lee et al. revealed that membrane permeability was decreased when swelling degree was increased (71). The silk fibroin film and the silk fibroin-collagen film in this study were added with glycerol into silk fibroin aqueous solution before casting into a film. The weight loss of both silk fibroin film and silk fibroin-collagen film might be affected by the solubility of glycerol in the film. According to Mariana F. Silva et al. reported that glycerol was highly soluble in water and could be leached from the films due to the immersion in water but still maintained their structural integrity and presented good handling properties (72). Another study reported that silk loss in mass greater than 50% after 42 days of in vitro degradation. But, silk could be degraded and resorbed in vivo over a longer time (typically within a year). The period of degradation degree test should be long enough to identify membrane degradation rate. Even if, the degradation degree of silk fibroin film and silk fibroin-collagen film were higher than collagen membrane, they could retain their initial structure better than collagen membrane.

Gross observation founded that all fabricated samples had transparent cloudy yellow color. They were not brittle and fragile at dry state. The bottom side of silk fibroin film and silk fibroin-collagen film had a smooth surface, while the top side had a non-homogeneous texture surface. Even if, the top side of silk fibroin film with collagen immobilization had a rougher surface but look smooth by gross observation. Measurement of surface topography or surface roughness by using atomic force microscopy (AFM) showed macroscale roughness (Ra; silk fibroin film = 0.1424  $\mu\text{m}$ , silk fibroin-collagen film = 0.2155  $\mu\text{m}$ ) on the top side of both fabricated membrane and nanoscale roughness (Ra; silk fibroin film = 0.0660  $\mu\text{m}$ , silk fibroin-collagen film = 0.0699  $\mu\text{m}$ ).

Depending on the scale of irregularities of the material surface, surface roughness can be divided into macro-roughness (100  $\mu\text{m}$  – millimeters), microroughness (100 nm – 100  $\mu\text{m}$ ) and nanoroughness (less than 100 nm), each with its specific influence. The response of cells to roughness is different depending on the cell type. Macroscopic descriptions of the surface roughness could be reasonable for osteoblasts adhesion (73). Primary rat osteoblasts had higher proliferation, alkaline phosphatase (ALP) activity and osteocalcin expression on the rough surface in comparison with smooth one (74). According to Oleh Andrukhov et al. reported that surfaces with microroughness values of 1–2  $\mu\text{m}$  seem to be suitable for osteoblast differentiation (75). Neither proliferation nor differentiation of osteoblasts appears to be supported by surfaces with higher or lower values. So, both fabricated membranes might support osteoblast proliferation and differentiation. Moreover, collagen which was immobilized on silk fibroin film surface might help osteoblasts cell attachment. According to Thomas C et al. reported that collagen itself had no ability to bind osteoinductive factors but could bind extracellular matrix proteins which had a high affinity for binding bone morphogenetic proteins, transforming growth factors, insulin-like growth factors and fibroblast growth factors (76). It was possible that several osteoinductive factors would be trapped by collagen fibers of the barrier membrane. Lahiji A. et al. reported that type I collagen could play an important role in osteoblastic differentiation (77). From this study, there was no porosity on both sides by gross observation. These surfaces would keep barrier function and prevented fibroblasts ingrowth into the bone defect. The porosity of the GBR membrane was an important property which affects the degree of bone regeneration beneath the membrane. Porosity could facilitate the diffusion of fluids, oxygen, nutrients, and substances which could support bone regeneration. However, the pore size should be proper for occlusive of faster-growing cells such as epithelial cells and gingival fibroblasts. Larger pore size also was an easy pathway for bacterial infiltration. In contrast, small pore size could limit the collagen deposition, the vascularization, and formation of a vascular tissue (78). The study in rat calvaria defect compared the efficacy of different pore size between perforated non-resorbable barrier membrane with different porosities (10, 25, 50, 75, 100, and 300  $\mu\text{m}$ ) and non-perforated barrier membrane on guided bone regeneration. The slow rate of new bone formation was related to the totally occlusive barrier membrane. In contrast, using perforated polyester meshes with exceeding 10  $\mu\text{m}$  pore size resulted in a faster rate of bone regeneration than perforated polyester meshes with 10  $\mu\text{m}$  pores were used. They concluded that the porosity of the barrier membrane was an important factor in the non-resorbable type of barrier membrane (79). So, there was no porosity of fabricated membrane in this study might not affect guided bone regeneration because the fabricated membrane could be resorbed according to another study which reported that resorption time might affect the

resorbable membrane on guiding hard tissue formation dominantly (80). Dietmar W et al. also reported that silk fibroin could act as an enzyme immobilization matrix with good mechanical properties and had blood compatibility and well-dissolved oxygen permeability in the wet state (81). Bio-Gide<sup>®</sup> (Geistlich Pharma, Switzerland), one of the most popular commercial non-crosslinked collagen membrane, was composed of porcine type I and type III collagen fibers. It was a bilayer membrane with an outer dense smooth layer and an inner porous layer. When Bio-Gide<sup>®</sup> was used for guided bone regeneration (GBR), an outer dense smooth layer was designed to prevent the invasion of fibroblasts in a membrane-protected bone defect while the inner porous layers could enable osteogenic cell migration to make bone ingrowth possible (82). Surface topography or surface roughness of the barrier membrane was another important factor influencing cell adhesion and behavior. Indeed, roughness modulates the biological response of tissues in contact with the barrier membrane.

The silk fibroin film which had hydrophilic macro-roughness surface tend to support MC3T3-E1 cell attachment better than the silk fibroin-collagen film which had hydrophobic microroughness surface. The SEM examination of the present study, cell attachment of MC3E3-T1 showed that osteoblast-like cells with several filopodias adhered to silk fibroin and commercial collagen membrane. While flat MC3E3-T1 cells with some filopodias were found on silk fibroin-collagen film. The hydrophilic or hydrophobic surface would also affect osteoblast attachment. In this study, the silk fibroin film showed a hydrophilic surface which was related to MC3T3-E1 cells attachment on the membrane. According to Wei et al. reported that osteoblast adhesion was decreased when the contact angle of the surface was increased (83). On the other hand, hydrophobic surfaces tend to bind more protein (84).

Regarding the water contact angle, the hydrophobic surface refers to a surface which had a water contact angle of more than 90° and the hydrophilic surface refers to a surface which had a water contact angle of less than 90°. This study founded that the water contact angle on silk fibroin film surface (76°) less than a silk fibroin film with collagen immobilization surface (112°) which showed more hydrophobicity. Wei et al. reported that osteoblast adhesion was decreased when the contact angle of the surface was increased (83). Therefore, silk fibroin film without collagen immobilization surface should be placed against the bone defect for osteoblast cells attachment and the silk fibroin with collagen immobilization should be lied against soft tissue. According to cell attachment, it was affected by lots of factors, such as cell behavior, material surface properties, and the environment. So, material surface properties should have proper hydrophobicity, charge, softness,

roughness and chemical composition of the biomaterial for influencing cell attachment. Chemical cross-linking between silk fibroin and collagen could result in hydrogen bonding formation. This observation could be explained that the N-H group of collagen binding reduced higher polarity of the carboxyl group in the glutamic acids of silk chain. This reaction might cause the hydrophobic surface of the new barrier membrane which had immobilized collagen on silk fibroin film when compared with another side which had no collagen immobilization.

While silk fibroin-collagen film had a hydrophobic surface, which might be affected by EDC/NHS cross-linking reaction. According to Chulhun Park et al. reported that the EDC/NHS reaction increase the hydrophobic interaction between the gelatin molecule (57). This study used chemical cross-linking with low toxic chemical substance, which was 1-Ethyl-3-(3-dimethylaminopropyl)-1-carbodiimide (EDC) and N-hydroxysuccinimide (NHS). The EDC/NHS chemical crosslink induced the formation of an amide bond by activation of the side chain carboxylic acid group afterward occurred aminolysis of the intermediates by the amino groups, which presented in the formation of interhelical cross-linking. The EDC/NHS chemical cross-linking induced collagen molecules by the formation of isopeptides without getting itself incorporated into the macromolecule as shown in *Figure 37*. This process could cross-link and random self-assembly of collagen immobilization on the silk fibroin film surface which was treated with EDC/NHS. The influence organization of self-assembling collagen fibrils on the silk fibroin surface was affected by pH, temperature, electrical gradients, stress mechanic and concentration (57). Moreover, the by-product of the cross-linking reaction was urea which can be easily removed during the routine rinsing process. So, this cross-linking method might be safe for membrane fabrication process due to MC3T3-E1 could attach on membrane surface 6 hours after cell seeding and maintain their viability for proliferation and differentiation. However, EDC/NHS was reported to be non-cytotoxic. In vitro and in vivo biocompatibility was observed in that studies. Osteoblasts cells could also attach, proliferate and differentiate on silk fibroin-collagen film. This present study showed that all study groups had a similar pattern of cell proliferation that increased over time. While mineralization assay founded graph pattern increased with time in silk fibroin and silk-fibroin collagen film groups. Interestingly that collagen membrane groups, optical density was the highest at Day 21 then decreased at Day 28. This study supported Altman et al. (14) that silk fibroin fibers supported the attachment, growth, and differentiation of adult human progenitor bone marrow stromal cells.

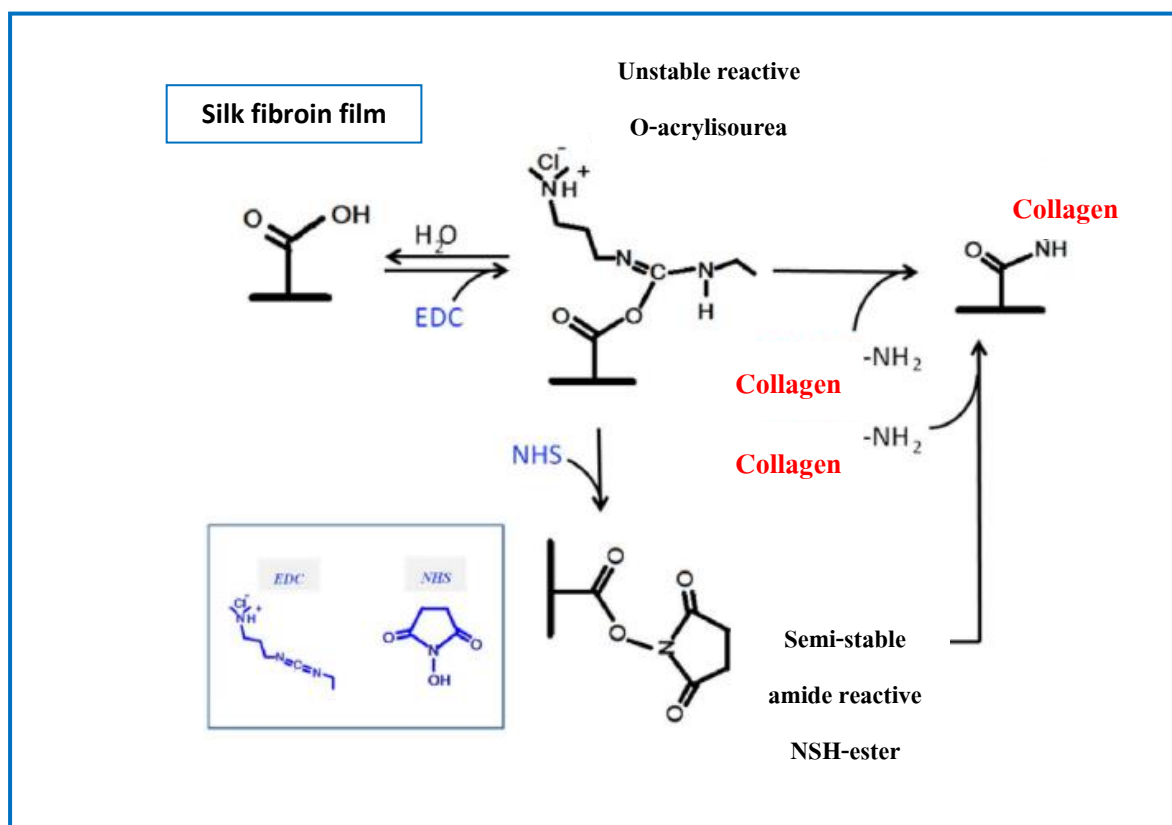


**Figure 37.** Reaction scheme for the surface modification of silk fibroin film by the collagen solution (57).

Evaluation of cell proliferation founded that the levels of optical density (OD) of MC3T3-E1 cells increased with the time in all experimental groups referred that both silk fibroin film and silk fibroin-collagen film had an ability to maintain cell viability and cell proliferation. Regards of the mineralization assay, measured by Alizarin Red S staining to evaluate mineralization in late osteoblast differentiation, founded that OD of both silk fibroin film and silk fibroin-collagen film increased with time and were highest on Day 28. While collagen membrane showed the highest values of mineralization on Day 21 and then decreased to the same level of silk-based on Day 28. It was well accepted that cells may interact with the substrate via chemical, physical and topological surface parameters, which played an essential role in the biocompatibility of biomaterials. The main challenge of fabricated resorbable barrier membranes is to match its resorption time with the periods of tissue formation. The structural integrity of the membrane should be maintained more than 4-6 months for GBR to support the new bone formation and maturation of the newly formed tissue (85). Selection and combination of appropriate biomaterial were important to achieve ideal barrier membrane properties. So, proper physical and mechanical properties of the resorbable membrane should be accompanied with good biocompatibility properties.

The silk fibroin film and silk fibroin-collagen film were successfully fabricated with simple materials. They were biocompatible, softened after soaking with distilled water, easily handling and able to be trimmed to adapt the defects. Further study of in vivo biocompatibility, barrier membrane efficacy, integration with tissues and body immune response should be further studied in the next phase.

## **CHAPTER 5**

### **CONCLUSION**

The in-house silk fibroin film and silk fibroin-collagen film had been fabricated at an economic cost and possess the properties of barrier membranes used for guided bone regeneration. The films could be trimmed, adjusted and softened by soaking in distilled water. Moreover, both fabricated films showed cellular affinity and biocompatibility for supporting osteoblast cells attachment, proliferation, and differentiation. Degradation degree of fabricated films was still not definite and the course of time testing should be longer than 28 days.

Further study on biocompatibility and the barrier efficacy *in vivo* should be performed to ensure the results before using in clinical practice.

## REFERENCES

1. Schenk RK, Buser D, Hardwick WR, Dahlin C. Healing pattern of bone regeneration in membrane-protected defects: a histologic study in the canine mandible. *Int J Oral Maxillofac Implants*. 1994; 9(1): 13-29.
2. Buser D, Dula K, Hirt HP, Schenk RK. Lateral ridge augmentation using autografts and barrier membranes: a clinical study with 40 partially edentulous patients. *J Oral Maxillofac Surg*. 1996; 54(4): 420-32; discussion 32-3.
3. Zitzmann NU, Naef R, Scharer P. Resorbable versus nonresorbable membranes in combination with Bio-Oss for guided bone regeneration. *Int J Oral Maxillofac Implants*. 1997; 12(6): 844-52.
4. Simion M, Baldoni M, Rossi P, Zaffe D. A comparative study of the effectiveness of e-PTFE membranes with and without early exposure during the healing period. *Int J Periodontics Restorative Dent*. 1994; 14(2): 166-80.
5. Gher ME, Quintero G, Assad D, Monaco E, Richardson AC. Bone grafting and guided bone regeneration for immediate dental implants in humans. *J Periodontol*. 1994; 65(9): 881-91.
6. Augthun M, Yildirim M, Spiekermann H, Biesterfeld S. Healing of bone defects in combination with immediate implants using the membrane technique. *Int J Oral Maxillofac Implants*. 1995; 10(4): 421-8.
7. Chattopadhyay S, Raines RT. Review collagen-based biomaterials for wound healing. *Biopolymers*. 2014; 101(8): 821-33.
8. Ferreira AM, Gentile P, Chiono V, Ciardelli G. Collagen for bone tissue regeneration. *Acta Biomater*. 2012; 8(9): 3191-200.
9. Miller N, Penaud J, Foliguet B, Membre H, Ambrosini P, Plombas M. Resorption rates of 2 commercially available bioresorbable membranes. A histomorphometric study in a rabbit model. *J Clin Periodontol*. 1996; 23(12): 1051-9.
10. Zhao S, Pinholt EM, Madsen JE, Donath K. Histological evaluation of different biodegradable and non-biodegradable membranes implanted subcutaneously in rats. *J Craniomaxillofac Surg*. 2000; 28(2): 116-22.
11. Hürzeler MB, Kohal RJ, Naghshbandl J, Mota LF, Conrath J, Hutmacher D, et al. Evaluation of a new bioresorbable barrier to facilitate guided bone regeneration around exposed implant



- threads: An experimental study in the monkey. *Int J Oral Maxillofac Surg*. 1998; 27(4): 315-20.
12. Von Arx T, Broggini N, Jensen SS, Bornstein MM, Schenk RK, Buser D. Membrane durability and tissue response of different bioresorbable barrier membranes: a histologic study in the rabbit calvarium. *Int J Oral Maxillofac Implants*. 2005; 20(6): 843-53.
  13. Rothamel D, Schwarz F, Sager M, Hertel M, Sculean A, Becker J. Biodegradation of differently cross-linked collagen membranes: an experimental study in the rat. *Clin Oral Implants Res*. 2005; 16(3): 369-78.
  14. Altman GH, Diaz F, Jakuba C, Calabro T, Horan RL, Chen J, et al. Silk-based biomaterials. *Biomaterials*. 2003; 24(3): 401-16.
  15. Samal SK, Dash M, Shelyakova T, Declercq HA, Uhlarz M, Banobre-Lopez M, et al. Biomimetic magnetic silk scaffolds. *ACS Appl Mater Interfaces*. 2015; 7(11): 6282-92.
  16. Kuboyama N, Kiba H, Arai K, Uchida R, Tanimoto Y, Bhawal UK, et al. Silk fibroin-based scaffolds for bone regeneration. *J Biomed Mater Res*. 2013; 101(2): 295-302.
  17. Rockwood DN, Preda RC, Yucel T, Wang X, Lovett ML, Kaplan DL. Materials fabrication from Bombyx mori silk fibroin. *Nat Protoc*. 2011; 6(10): 1612-31.
  18. Zhang X, Reagan MR, Kaplan DL. Electrospun silk biomaterial scaffolds for regenerative medicine. *Adv Drug Deliv Rev*. 2009; 61(12): 988-1006.
  19. Wang Y, Kim H-J, Vunjak-Novakovic G, Kaplan DL. Stem cell-based tissue engineering with silk biomaterials. *Biomaterials*. 2006; 27(36): 6064-82.
  20. Yeelack W, BSaMJ. A mimicked collagen layer/silk fibroin film as a cardio patch scaffold. *Bioinspir Biomim Nan*. 2014; 3(BBN4): 1-11.
  21. Vepari C, Kaplan DL. Silk as a biomaterial. *Prog Polym Sci*. 2007; 32(8-9): 991-1007.
  22. Kim J-Y, Yang B-E, Ahn J-H, Park SO, Shim H-W. Comparable efficacy of silk fibroin with the collagen membranes for guided bone regeneration in rat calvarial defects. *J Adv Prosthodont*. 2014; 6(6): 539-46.
  23. Elgali I, Omar O, Dahlin C, Thomsen P. Guided bone regeneration: materials and biological mechanisms revisited. *Eur J Oral Sci*. 2017; 125(5): 315-37.
  24. Wang HL, Carroll MJ. Guided bone regeneration using bone grafts and collagen membranes. *Quintessence Int*. 2001; 32(7): 504-15.
  25. Michael M, Bornstein TvA, Dieter D, Bosshardt. Properties of Barrier Membrane. *20 Years of Guided Bone Regeneration in implant Dentistry*. 2009: 47-69.

26. Benic GI, Hammerle CH. Horizontal bone augmentation by means of guided bone regeneration. *J Periodontol.* 2000. 2014; 66(1): 13-40.
27. Dimitriou R, Mataliotakis GI, Calori GM, Giannoudis PV. The role of barrier membranes for guided bone regeneration and restoration of large bone defects: current experimental and clinical evidence. *BMC Med.* 2012; 10: 81.
28. Wessing B, Urban I, Montero E, Zechner W, Hof M, Alandez Chamorro J, et al. A multicenter randomized controlled clinical trial using a new resorbable non-cross-linked collagen membrane for guided bone regeneration at dehiscenced single implant sites: interim results of a bone augmentation procedure. *Clin Oral Implants Res.* 2017; 28(11): e218-e26.
29. Dahlin C, Sennerby L, Lekholm U, Linde A, Nyman S. Generation of new bone around titanium implants using a membrane technique: an experimental study in rabbits. *Int J Oral Maxillofac Implants.* 1989; 4(1): 19-25.
30. Dahlin C, Linde A, Gottlow J, Nyman S. Healing of bone defects by guided tissue regeneration. *Plast Reconstr Surg.* 1988; 81(5): 672-6.
31. Buser D, Bragger U, Lang NP, Nyman S. Regeneration and enlargement of jaw bone using guided tissue regeneration. *Clin Oral Implants Res.* 1990; 1(1): 22-32.
32. Zitzmann NU, Scharer P, Marinello CP. Long-term results of implants treated with guided bone regeneration: a 5-year prospective study. *Int J Oral Maxillofac Implants.* 2001; 16(3): 355-66.
33. Jung RE, Fenner N, Hammerle CH, Zitzmann NU. Long-term outcome of implants placed with guided bone regeneration (GBR) using resorbable and non-resorbable membranes after 12-14 years. *Clin Oral Implants Res.* 2013; 24(10): 1065-73.
34. Becker W, Dahlin C, Becker BE, Lekholm U, van Steenberghe D, Higuchi K, et al. The use of e-PTFE barrier membranes for bone promotion around titanium implants placed into extraction sockets: a prospective multicenter study. *Int J Oral Maxillofac Implants.* 1994; 9(1): 31-40.
35. Pati F, Datta P, Adhikari B, Dhara S, Ghosh K, Das Mohapatra PK. Collagen scaffolds derived from fresh water fish origin and their biocompatibility. *J Biomed Mater Res A.* 2012; 100(4): 1068-79.
36. Nagai N, Nakayama Y, Zhou YM, Takamizawa K, Mori K, Munekata M. Development of salmon collagen vascular graft: mechanical and biological properties and preliminary implantation study. *J Biomed Mater Res B Appl Biomater.* 2008; 87(2): 432-9.

37. Lee JY, Hall R, Pelinkovic D, Cassinelli E, Usas A, Gilbertson L, et al. New use of a three-dimensional pellet culture system for human intervertebral disc cells: initial characterization and potential use for tissue engineering. *Spine J.* 2001; 26(21): 2316-22.
38. Debby Hwang MS. Guided bone regeneration: Concepts and materials. *Implant Site Development.* 2012: 153-78.
39. Sadowska M, Kołodziejewska I, Niecikowska C. Isolation of collagen from the skins of Baltic cod (*Gadus morhua*). *Food Chem.* 2003; 81(2): 257-62.
40. Nagai N, Yunoki S, Suzuki T, Sakata M, Tajima K, Munekata M. Application of cross-linked salmon atelocollagen to the scaffold of human periodontal ligament cells. *J Biosci Bioeng.* 2004; 97(6): 389-94.
41. Lee SW, Kim SG. Membranes for the Guided Bone Regeneration. *Plast Reconstr Surg.* 2014; 36(6): 239-46.
42. Shimura K, Kikuchi A, Ohtomo K, Katagata Y, Hyodo A. Studies on silk fibroin of *Bombyx mori*. I. Fractionation of fibroin prepared from the posterior silk gland. *J Biochem.* 1976; 80(4): 693-702.
43. Minoura N, Tsukada M, Nagura M. Physico-chemical properties of silk fibroin membrane as a biomaterial. *Biomaterials.* 1990; 11(6): 430-4.
44. Zhou J, Zhang B, Shi L, Zhong J, Zhu J, Yan J, et al. Regenerated silk fibroin films with controllable nanostructure size and secondary structure for drug delivery. *ACS Appl Mater Interfaces.* 2014; 6(24): 21813-21.
45. Demura M, Asakura T. Immobilization of glucose oxidase with *Bombyx mori* silk fibroin by only stretching treatment and its application to glucose sensor. *Biotechnol Bioeng.* 1989; 33(5): 598-603.
46. Lu Q, Hu X, Wang X, Kluge JA, Lu S, Cebe P, et al. Water-insoluble silk films with silk I structure. *Acta Biomater.* 2010; 6(4): 1380-7.
47. Volkov V, Ferreira Ana V, Cavaco-Paulo A. On the Routines of Wild-Type Silk Fibroin Processing Toward Silk-Inspired Materials: A Review. *Macromol Mater Eng.* 2015; 300(12): 1199-216.
48. Kim KH, Jeong L, Park HN, Shin SY, Park WH, Lee SC, et al. Biological efficacy of silk fibroin nanofiber membranes for guided bone regeneration. *J Biotechnol.* 2005; 120(3): 327-39.
49. Rahman M, Brazel CS. The plasticizer market: an assessment of traditional plasticizers and research trends to meet new challenges. *Prog Polym Sci.* 2004; 29(12): 1223-48.

50. Zhang H, Deng L, Yang M, Min S, Yang L, Zhu L. Enhancing Effect of Glycerol on the Tensile Properties of Bombyx mori Cocoon Sericin Films. *Int J Mol Sci*. 2011; 12(5): 3170-81.
51. Mariana F. Silva MAdM, Grí 'nia M. Nogueira, Andrea C. D. Rodas, Olga Z. Higa, Marisa M. Beppu. Glycerin and Ethanol as Additives on Silk Fibroin Films: Insoluble and Malleable Films. *J Appl Polym Sci*. 2012; 128: 115–22.
52. Sudo H, Kodama HA, Amagai Y, Yamamoto S, Kasai S. In vitro differentiation and calcification in a new clonal osteogenic cell line derived from newborn mouse calvaria. *The J Cell Biol*. 1983; 96(1): 191-8.
53. Wang D, Christensen K, Chawla K, Xiao G, Krebsbach PH, Franceschi RT. Isolation and characterization of MC3T3-E1 preosteoblast subclones with distinct in vitro and in vivo differentiation/mineralization potential. *J Bone Miner Res*. 1999; 14(6): 893-903.
54. Quarles LD, Yohay DA, Lever LW, Caton R, Wenstrup RJ. Distinct proliferative and differentiated stages of murine MC3T3-E1 cells in culture: an in vitro model of osteoblast development. *J Bone Miner Res*. 1992; 7(6): 683-92.
55. Grigoriadis AE, Petkovich PM, Ber R, Aubin JE, Heersche JN. Subclone heterogeneity in a clonally-derived osteoblast-like cell line. *Bone*. 1985; 6(4): 249-56.
56. Benjakul S, Thiansilakul Y, Visessanguan W, Roytrakul S, Kishimura H, Prodpran T, et al. Extraction and characterisation of pepsin-solubilised collagens from the skin of bigeye snapper (*Priacanthus tayenus* and *Priacanthus macracanthus*). *J Sci Food Agric*. 2010; 90(1): 132-8.
57. Park C, Vo CL, Kang T, Oh E, Lee BJ. New method and characterization of self-assembled gelatin-oleic nanoparticles using a desolvation method via carbodiimide/N-hydroxysuccinimide (EDC/NHS) reaction. *Eur J Pharm Biopharm*. 2015; 89: 365-73.
58. Clark Science Center. Available from:  
<http://www.science.smith.edu/cmi/wpcontent/uploads/sites/26/2015/06/quanta-recolored.jpg>
59. University of Wisconsin. Available from:  
<https://www.uwlax.edu/csh/instrumentation-resources/spectroscopy/>
60. Dataphysics Instruments. Available from:  
<https://www.dataphysics-instruments.com/products/oca/>
61. Norwegian University of Science and Technology. Available from:  
<https://www.ntnu.no/nano/renrom/utstyr/afmnanosurf>

62. Elis Electronic Instruments & Systems. Available from: <http://www.elis.it/lloyd-pdf/LRXPlus.pdf>
63. Shu-Tung Li H-CC, Natsuyo Shishido Lee, Rushali Ringshia and Debbie Yuen. A Comparative Study Of Zimmer BioMend® And BioMend® Extend™ Membranes Made At Two Different Manufacturing Facilities. 2013.
64. Kawase M, Hayashi T, Asakura M, Mieki A, Fuyamada H, Sassa M, et al. Cell Proliferation Ability of Mouse Fibroblast-Like Cells and Osteoblast-Like Cells on a Ti-6Al-4V Alloy Film Produced by Selective Laser Melting. *Mater Sci Appl*. 2014; Vol.05No.07: 9.
65. Li T-T, Ebert K, Vogel J, Groth T. Comparative studies on osteogenic potential of micro- and nanofibre scaffolds prepared by electrospinning of poly( $\epsilon$ -caprolactone). *Biomaterials*. 2013; 2(1): 13.
66. Krimm S, Bandekar J. Vibrational spectroscopy and conformation of peptides, polypeptides, and proteins. *Adv Protein Chem Struct Biol*. 1986; 38: 181-364.
67. Abe Y, Krimm S. Normal vibrations of crystalline polyglycine I. *Biopolymers*. 1972; 11(9): 1817-39.
68. Kittiphattanabawon P, Benjakul S, Visessanguan W, Shahidi F. Isolation and characterization of collagen from the cartilages of brownbanded bamboo shark (*Chiloscyllium punctatum*) and blacktip shark (*Carcharhinus limbatus*). *J Food Sci Technol*. 2010; 43(5): 792-800.
69. Marouf HA, El-Guindi HM. Efficacy of high-density versus semipermeable PTFE membranes in an elderly experimental model. *Oral Surg Oral Med Oral Pathol Oral Radiol Endod*. 2000; 89(2): 164-70.
70. Song JH, Kim HE, Kim HW. Collagen-apatite nanocomposite membranes for guided bone regeneration. *J Biomed Mater Res B Appl Biomater*. 2007; 83(1): 248-57.
71. Lee Y-J, An S-J, Bae E-B, Gwon H-J, Park J-S, Jeong SI, et al. The Effect of Thickness of Resorbable Bacterial Cellulose Membrane on Guided Bone Regeneration. *Materials*. 2017; 10(3): 320.
72. Silva MF, de Moraes MA, Nogueira GM, Rodas ACD, Higa OZ, Beppu MM. Glycerin and ethanol as additives on silk fibroin films: Insoluble and malleable films. *J Appl Polym Sci*. 2012; 128(1): 115-22.
73. Donoso MG, Méndez-Vilas A, Bruque JM, González-Martin ML. On the relationship between common amplitude surface roughness parameters and surface area: Implications for the study of cell-material interactions. *Int Biodeterior Biodegradation*. 2007; 59(3): 245-51.

74. Hatano K, Inoue H, Kojo T, Matsunaga T, Tsujisawa T, Uchiyama C, et al. Effect of surface roughness on proliferation and alkaline phosphatase expression of rat calvarial cells cultured on polystyrene. *Bone*. 1999; 25(4): 439-45.
75. Andrukhov O, Huber R, Shi B, Berner S, Rausch-Fan X, Moritz A, et al. Proliferation, behavior, and differentiation of osteoblasts on surfaces of different microroughness. *Dent Mater*. 2016; 32(11): 1374-84.
76. Chandy T, Sharma CP. Chitosan--as a biomaterial. *Trends Biomater Artif Organs*. 1990; 18(1): 1-24.
77. Lahiji A, Sohrabi A, Hungerford DS, Frondoza CG. Chitosan supports the expression of extracellular matrix proteins in human osteoblasts and chondrocytes. *J Biomed Mater Res A*. 2000; 51(4): 586-95.
78. Taylor DF, Smith FB. Porous methyl methacrylate as an implant material. *J Biomed Mater Res A*. 1972; 6(1): 467-79.
79. Lundgren A, Lundgren D, Taylor A. Influence of barrier occlusiveness on guided bone augmentation. An experimental study in the rat. *Clin Oral Implants Res*. 1998; 9(4): 251-60.
80. Rakhmatia YD, Ayukawa Y, Furuhashi A, Koyano K. Current barrier membranes: titanium mesh and other membranes for guided bone regeneration in dental applications. *J Prosthodont Res*. 2013; 57(1): 3-14.
81. Hutmacher DW. Scaffolds in tissue engineering bone and cartilage. *Biomaterials*. 2000; 21(24): 2529-43.
82. Schlegel AK, Möhler H, Busch F, Mehl A. Preclinical and clinical studies of a collagen membrane (Bio-Gide®). *Biomaterials*. 1997; 18(7): 535-8.
83. Wei J, Igarashi T, Okumori N, Igarashi T, Maetani T, Liu B, et al. Influence of surface wettability on competitive protein adsorption and initial attachment of osteoblasts. *Biomed Mater*. 2009; 4(4): 045002.
84. Protein-Surface Interactions. An Introduction To Tissue-Biomaterial Interactions.
85. Kozlovsky A, Aboodi G, Moses O, Tal H, Artzi Z, Weinreb M, et al. Bio-degradation of a resorbable collagen membrane (Bio-Gide) applied in a double-layer technique in rats. *Clin Oral Implants Res*. 2009; 20(10): 1116-23.

## VITAE

**Name** Miss Chanokpim Chankum

**Student ID** 5910820005

### **Educational Attainment**

<b>Degree</b>	<b>Name of Institution</b>	<b>Year of Graduation</b>
Higher Graduate Diploma in Clinical Science (Oral and Maxillofacial Surgery)	Prince of Songkla University	2015
Doctor of Dental Surgery	Chiang Mai University	2012

### **Work-Position and Address**

The Dental public health, Sukhothai provincial health office, Sukhothai, Thailand, 64000

### **List of Publication and Proceeding**

Chankum C., Pripatnanont P., Meesane J. Characterization of a New Silk Fibroin-Fish Collagen Barrier Membrane. 4<sup>th</sup> Bangkok International Implant Symposium. 2017.